ARTICLE

Recent advances in continuous-flow organocatalysis for process intensification

Received 00th January 20xx,
Accepted 00th January 20xx

DOI: 10.1039/x0xx00000x

Carmela De Risi,* Olga Bortolini, Arianna Brandolese, Graziano Di Carmine, Daniele Ragno and Alessandro Massi*

Chemistry in continuous-flow continues to attract attention from the community of synthetic organic chemists due to its now well-recognized benefits including, inter alia, quick reaction times, operational safety, rapid reaction screening/optimization, enhanced automation with possible addition of in-line reaction analysis, and easy scalability. Coupling of flow chemistry to enabling technologies (e.g. unconventional solvents, supported reagents or catalysts, microwave irradiation, photochemistry, inductive heating, microreactors) as well as to additive manufacturing (AM) technologies (i.e. 3D printing) gives additional advantages for throughput and automation, and besides this, unique opportunities are offered by compartmentalization, that allows multistep syntheses to occur reconciling incompatible reaction conditions. Based on all this, continuous-flow may itself be seen as an enabling technology which leads in the direction of process intensification meeting increasingly pressing sustainability issues (e.g. waste minimization, cost/energy reduction). As part of flow chemistry, organocatalysis represents an active research area under which there is large opportunity for re-optimizing long-standing reactions or inventing new transformations. Both homogeneous (soluble) and heterogeneous (insoluble) organic molecules have been used as catalysts for continuous-flow processing in either achiral or asymmetric fashion, any issue inherent to a homogeneous approach (high catalyst loading, difficult catalyst separation) being typically overcome with the use of heterogenized organocatalysts. This review is aimed to cover the progresses on organocatalysis in continuous-flow from 2016 to the end of 2019, with special attention paid to the comparison between batch and flow processes for each discussed transformation to substantiate the potential of flow technology for process intensification.

1. Introduction

The last two decades have seen a constantly growing attention to the application of continuous-flow processes[1] for syntheses as a result of the many benefits offered by this enabling technology[2] in comparison to batch chemistry. These include, among others, shorter reaction times, improved surface to volume ratios and much faster mixing, operational safety (superior heat and mass transfer, smaller quantity of reactants/solvents), easy and rapid reaction screening and optimization (real-time control of reaction parameters), improved automation (on-demand process monitoring by incorporated in-line equipments), and enhanced scalability.
In addition, the continuous-flow strategy offers unique opportunities in multistep reaction sequences through compartmentalization, which allows for conflicting reaction conditions to occur in cascade mode.

But it is also important that flow chemistry can be joined to other enabling technologies (e.g. microwave irradiation, inductive heating, supported reagents or catalysts, photochemistry, unconventional solvents) so that there is added advantage in terms of automation and throughput.[2]
Moreover, synergism between flow chemistry and additive manufacturing (AM) technologies has been recently demonstrated, 3D printing being able to create new scenarios in the field of synthetic organic transformations thanks to both fabrication and use of 3D printed flow reactors.[3] Beyond that, the impossible becomes possible using flow microreactors for "flash" chemistry, enabling reaction times to be extremely short (<1s) to realize those difficult (if not inconceivable) flask reactions.[4]
Ultimately, continuous-flow implies process intensification,[5] well addressing ever more pressing sustainability issues (e.g. energy and cost reduction, waste minimization).[6] In this regard, it must be said that the US Government Accountability Office (GAO) has included continuous processing between the three main technologies that ensure sustainable chemical production, along with catalysts and solvents that are not hazardous or derived from renewable resources.[7]
By combining aspects of both process optimization and process intensification, chemical processing in continuous-flow

[a] Dipartimento di Scienze Chimiche e Farmaceutiche, Via Luigi Borsari 46, I-44121 Ferrara, Italy.
[b] E-mail: alessandro.massi@unife.it, carmela.derisi@unife.it
† In memory of Prof. Cinzia Chiappe

provides a connection between lab chemistry and chemical engineering. So, continuous-flow microreactors that are used for transformations at the bench-scale may be seen as the small-scale version of industrial reactors, the optimized microflow reactions representing a good starting point for scale-up studies in the fine chemical industry towards safe, easily automated/monitored and sustainable production processes.[8]

In this context, continuous-flow manufacturing of Active Pharmaceutical Ingredients (API) has recently emerged as an active research area,[9,10] and both the U.S. Food and Drug Administration (FDA) and the European Medicines Agency (EMA) have prepared specific guidelines for the development of commercialized flow transformations in the pharmaceutical field.[11]

In the context of flow chemistry, organocatalysis[12] has caught attention since the end of 2000[13] and is still an ongoing topic which offers significant opportunities in terms of invention of new transformations or re-optimization of well-established reactions.

In analogy with flask-type procedures, organocatalyzed synthetic strategies in continuous-flow may be designed to occur in the presence of a homogeneous (soluble) catalyst, which is pumped into the reactor together with the reagent compounds (Figure 1A). However, both the high catalyst loading often necessary (10-20 mol%) and difficulties in recycling the organocatalyst have made it increasingly attractive the use of heterogenized (insoluble) organocatalysts, a simple solid/liquid separation from the reaction solution allowing for their recovery and subsequent re-use.

In this last case, the heterogeneous catalyst (Figure 1B) could be used *i)* as the filling material of a packed (fixed)-bed reactor (immobilization on polymeric or inorganic particles, e.g. silica gel), *ii)* in the form of monolithic column (copolymerization of different monomers, including one that contains the catalyst, inside the reactor), or *iii)* as a wall-coated reactor (covalent attachment onto the reactor internal walls).[14]

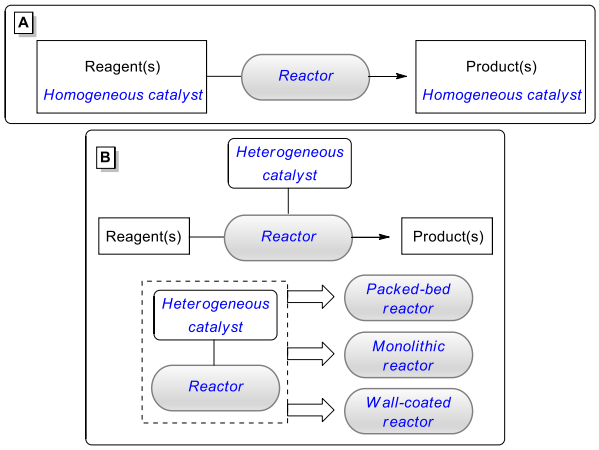

Fig. 1 Organocatalyzed synthetic strategies in continuous-flow. (A) Homogeneous approach. (B) Heterogeneous route.

Several reviews on the topic of catalysis in flow have appeared in the literature,[15] with four papers dedicated solely to organocatalysis that appeared in 2015.[16]

In this respect, Puglisi *et al.* surveyed stereoselective continuous-flow processes promoted by either supported or non-supported chiral organocatalysts together with some selected examples on the use of achiral organic molecules as catalysts,[16a] while Finelli *et al.*[16b] as well as Atodiresei *et al.*[16c] focused exclusively on asymmetric organocatalysis in continuous-flow (differentiating between homogeneous and heterogeneous reactions). Especially in the latter case, attention was placed on the differences between batch and flow approaches so as to highlight the advantages (disadvantages) of the continuous-flow production. Besides, the use of solid-supported chiral organocatalysts was covered by Pericàs research team.[16d]

Thenceforth, papers on continuous-flow organocatalysis have continued to appear, even on less common themes (e.g. polymer chemistry). And importantly, the majority of these works provided in-depth discussions on batch process optimization for a given transformation in preparation to the subsequent use of the flow methodology, offering a very broad view in terms of possible process intensification.

On that basis, we think that a further overview on application of continuous-flow technique in organocatalytic reactions could help give an up-to-date picture of this still current issue.

In this Minireview, we focused our attention on organocatalytic continuous-flow processes that have been reported in the literature from 2016 to the end of 2019.

In line with previous review articles, these contributions can be traced back to two main strategies, entailing the use of both chiral and achiral organic molecules as catalysts, as shown in Figure 2. This being the case, the literature data have been organized depending on whether the catalytic flow strategies were developed under homogeneous (Section 2) or heterogeneous (Section 3) conditions, with each strategy further detailed on the basis of the nature of the catalyst used (achiral *vs* chiral).

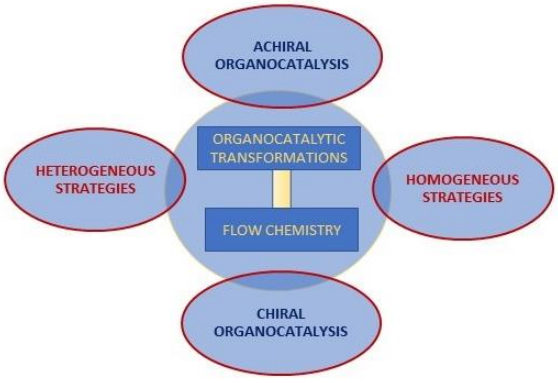

Fig. 2 Chart of the main strategies used in continuous-flow organocatalysis.

With the aim of framing the works discussed in a possible process intensification perspective, we have privileged some typical articles for which the flow process(es) could be effectively compared to the parent batch reaction(s). For added

precision, two major types of publications were chosen to fulfill this criterion, namely i) reports wherein a same reaction was studied under both batch and flow mode, and ii) papers that only described the continuous-flow process for a given transformation, eventually compared against known data of the equivalent batch approach.

Therefore, where possible, for each work presented we have detailed both the flow process and the preliminary optimization studies in batch conditions, then making a comparison of the two approaches. Otherwise, we paid attention to the continuous-flow transformation, limiting ourselves to comparing it with the corresponding (already known) batch reaction. We must also say that alongside process issues (e.g. reaction optimization, stability/recyclability of the heterogeneous catalysts, productivity/scalability in flow regime), if possible, specific chemical aspects were also highlighted, including mechanistic ones.

2. Homogeneous strategies

2.1 Homogeneous achiral organocatalysis

Both Lewis acids and Lewis bases found application in continuous-flow organocatalytic transformations.

In particular, acetalization of aldehydes was performed in the presence of tropylium salts as organic Lewis acid catalysts (Scheme 1).[17]

Optimization studies in batch system led to establish a general protocol for the reaction between aldehydes and trialkyl orthoformates in the presence of tropylium tetrafluoroborate ($TropBF_4$), giving access to a broad library of acetal derivatives (Scheme 1A).

It is likely that the acetalization reaction proceeds *via* the adduct **1** deriving from tropylium cation-aldehyde activation and subsequent nucleophilic addition with the orthoester (Scheme 1B). Either intramolecular or intermolecular alkyl group transfer paves the way to the fragmentation of **1** bringing to acetal precursor **2** along with alkyl formate by-product. Final loss of the tropylium ion from **2** concludes the catalytic cycle. However, it cannot be excluded that the reaction goes through activation of the orthoformate by tropylium ion.

The batch acetalization method promoted by tropylium ion was next performed in continuous-flow regime using the simple setup illustrated in Scheme 1C. The operating conditions were slightly different in comparison with the batch ones with regard to temperature and catalyst loading. Actually, higher temperature (90 °C) gave reduced residence (reaction) time (τ), and a smaller amount of the Lewis acid species (1 mol%) did not affect the anticipated results. At a flow rate (FR) of 0.1 mL/min, both aliphatic and aromatic aldehydes could be transformed in the corresponding acyclic acetals in up to 99% yield on the gram scale (up to 12 g).

Just as interesting is that the flow approach made possible to achieve acetalization of aldehydes using ethylene epoxide as the counterpart. This is a quite difficult task to perform in batch for the gaseous nature of this reagent.

Also noteworthy is that the catalyst did not suffer major changes in both batch and flow conditions. After reaction, it remained at ca. 90-100% of the starting loading and could be easily isolated (column chromatography or recrystallization) for re-use.

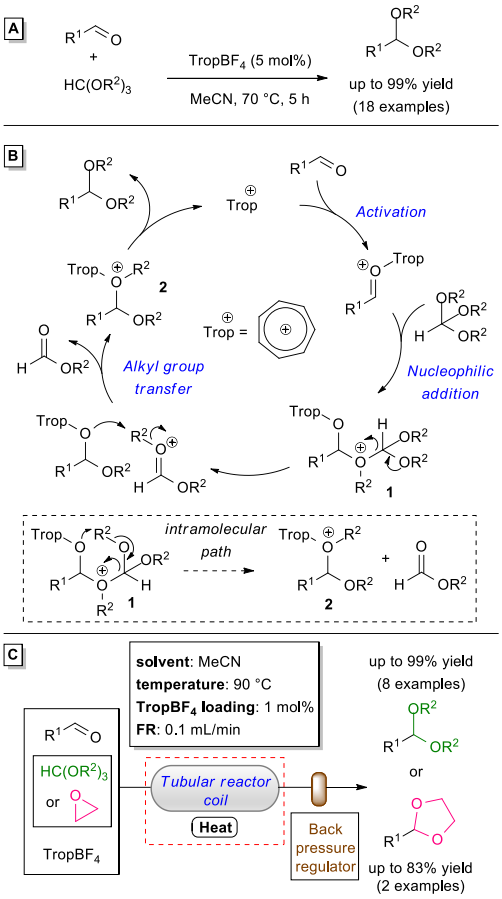

Scheme 1 Tropylium ion-catalyzed acetalization reaction. (A) Acetalization in batch system. (B) Tentative organocatalytic cycle. (C) Acetalization under continuous-flow.

Triphenylmethylium (tritylium) cation has shown effectiveness in catalyzing the diastereoselective synthesis of benzodihydropyran derivatives from salicylaldimines and electron-rich alkenes *via* interrupted Povarov reactions (Scheme 2).[18,19]

Very positive results have been reported for batch transformations using 2,3-dihydrofuran (DHF), ethyl vinyl ether and 1-vinylpyrrolidin-2-one as alkene substrates in the presence of tritylium tetrafluoroborate (TrBF4, 1 mol%) in THF solvent at room temperature, which produced the target products in excellent yield (up to 92%) and stereoselectivity (up to 95:5 cis/trans ratio) (Scheme 2A).

As depicted in Scheme 2B for the reaction between DHF and salicylaldimine, it was proposed that the latter is initially activated by tritylium ion to form intermediate **3** which is then intercepted by the nucleophilic alkene. The resulting species **4** participates in an intramolecular *O*-nucleophilic addition followed by an intramolecular proton transfer releasing the

tricyclic final compound with concomitant regeneration of the Lewis acid organocatalyst.

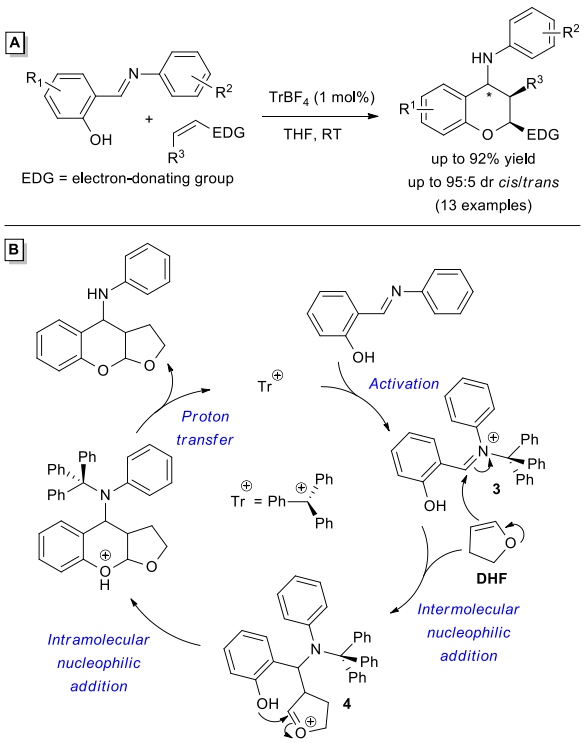

Scheme 2 Tritylium ion-catalyzed diastereoselective synthesis of benzodihydropyrans *via* interrupted Povarov reaction. (A) Reaction in batch conditions. (B) Assumed mechanistic pathway.

Due to intrinsic difficulties related to both preparation and handling of the imine starting materials, a one-pot, three component approach was implemented for the preparation of benzodihydropyran derivatives, involving reaction between anilines, salicylaldehyde and DHF (1 mol% $TrBF_4$, 4Å MS, THF, RT, 10 min) (Scheme 3A).

However, yields and diastereoselectivities were slightly lower, probably because of carbocation deactivation (decomposition) by water generated in the imine-forming step.

This problem has been circumvented by changing the one-pot batch method to a two-stage convergent continuous-flow strategy whereby dewatered salicylaldimine was preformed (Scheme 3B, *microreactor I/absorbent column*), and then reacted with tritylium ion/DHF solution (Scheme 3B, *microreactor II*).

Of note, the anticipated benzodihydropyran was obtained in 88% yield, 90:10 dr *cis*/*trans* and what's more, in a 10-fold reduced time (τ = 1 min).

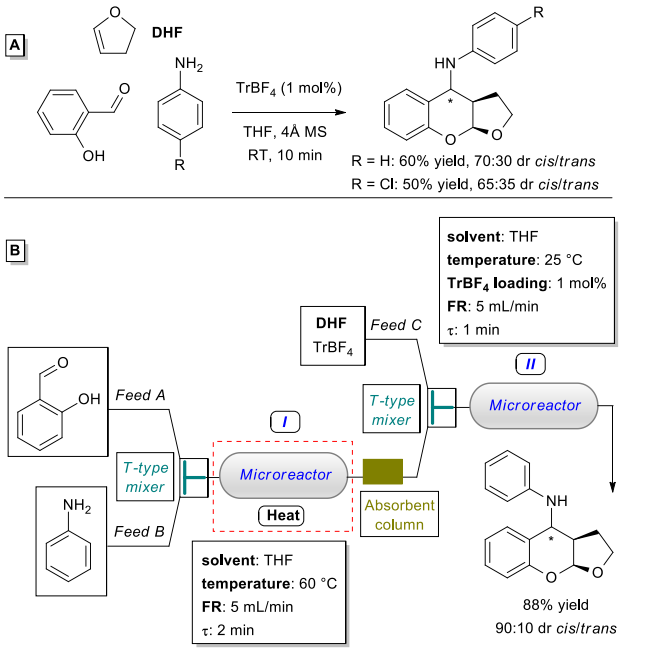

Scheme 3 Tritylium ion-catalyzed diastereoselective synthesis of benzodihydropyrans. (A) One-pot three component approach in batch mode. (D) Continuous-flow two-stage convergent synthesis of salicylaldimine-derived benzodihydropyran.

Di Marco *et al.* reported a straightforward continuous-flow procedure telescoping the generation of N-heterocyclic carbenes (NHCs) and their use as Lewis base organocatalysts[20] in benchmark transesterification and amidation reactions (Scheme 4).[21]

Initial studies on the model NHC-promoted transesterification between benzyl alcohol and vinyl acetate allowed the authors to design the microfluidic apparatus which is depicted in Scheme 4A. First, a imidazol(in)ium salt and potassium bis(trimethylsilyl)amide (KHMDS) solutions were carried to a capillary loop in which NHC formation took place (τ = 10 min). Exiting from the reactor, the NHC solution was then conveyed to an additional capillary loop joined by the equimolar mixture of alcohol and ester. The latter, for its part, was formed in a suitable premixing unit. The NHC-catalyzed transesterification went to completion within 10 min (1 mol% cat., FR = 0.1 mL/min) at room temperature, as confirmed by in-line infrared (IR) spectroscopy. To note is the fact that this system was used within 6 h with unchanged results and operational stability.

In-depth investigation have pointed out that conversions (yields) depended on both the nature of the NHC heterocyclic core and its *N*-substituents, similar to what happens in batch conditions.[22-24] In truth, aryl-substituted imidazolin-2-ylidenes gave the ester product in lower yields than the corresponding imidazol-2-ylidene derivatives, and *N*-mesitylene substituted imidazol-2-ylidene (IMes) catalyst furnished the best result in terms of conversion (> 99%) and yield (96%) after conventional work-up (collection, evaporation of the solvent, filtration on silica gel). Remarkably, further implementation could be achieved by in-line downstream quench/extraction/separation, provided that toluene was used as solvent at the stage of premixing.

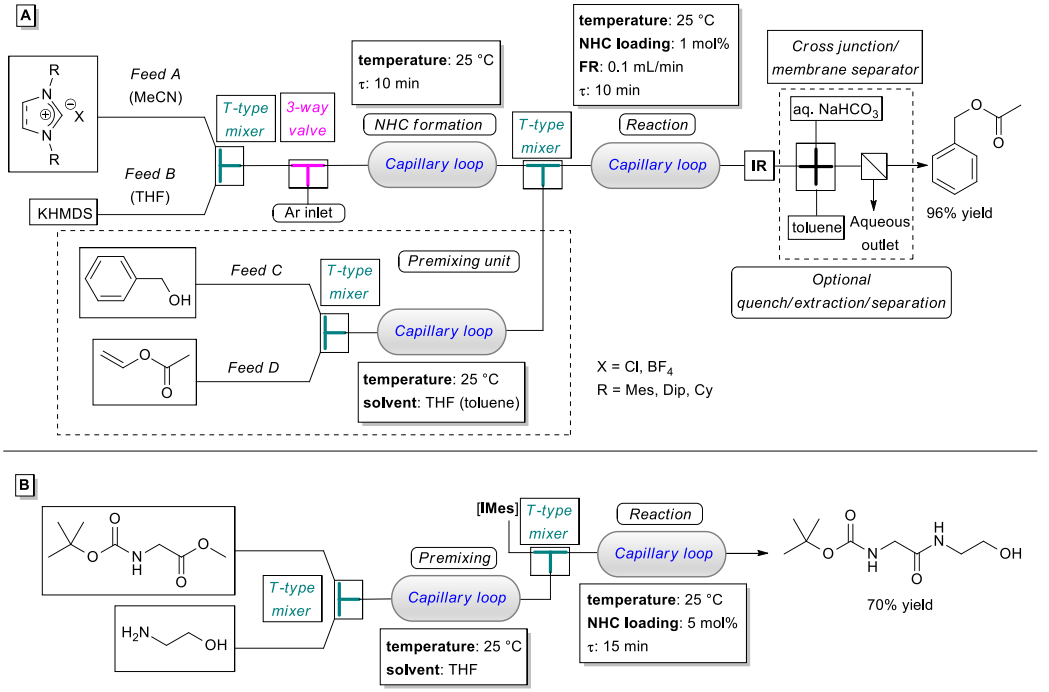

Scheme 4 (A) Continuous-flow apparatus for NHCs formation telescoped with NHC-catalyzed transesterification reaction. (B) Continuous-flow NHC-catalyzed amidation reaction.

Likewise, the optimal IMes catalyst was applied to achieve the amidation of *N*-Boc-glycine methyl ester with ethanolamine (Scheme 4B). Full conversion was fulfilled under somewhat modified experimental conditions (5 mol% cat., τ = 15 min) leading to the expected product in 70% isolated yield.

The organocatalytic α-trifluoromethylthiolation of silylenol ethers derived from unactivated ketones was achieved by the combined use of a trifluoromethylthiolating species and catalytic Lewis base (Scheme 5).[25]

Preliminary investigation in batch mode resulted in establishing tetrahydrothiophene (THT) as the best performing organocatalyst in combination with *N*-(trifluoromethylthio)saccharin, and best reaction conditions were those appearing in Scheme 5A. That way diverse α-trifluoromethylthiolated ketones have been produced in up to 75% conversion.

This procedure was developed further in continuous-flow at the optimal temperature of 60 °C (Scheme 5B). This regime gave better response in terms of reaction time (τ = 10 min), productivity (*P*) and space-time yield (STY), which were respectively 1.5 and 200 times higher than for the synthesis in flask.

Otherwise, for what concerns chemical efficiency, conversions were lower (up to 52%), and a not negligible decomposition of the silylenol ether reagent occurred at higher temperatures at the expense of product yield.

Very important was also the composition of the feeding solutions. The best option was to keep the solution of the trifluoromethylthiolating species separate from the one containing both the silylenol ether and the organocatalyst. It should be noted that the latter also included byphenyl (BPH) used as internal standard for monitoring conversions by gas-chromatography (GC).

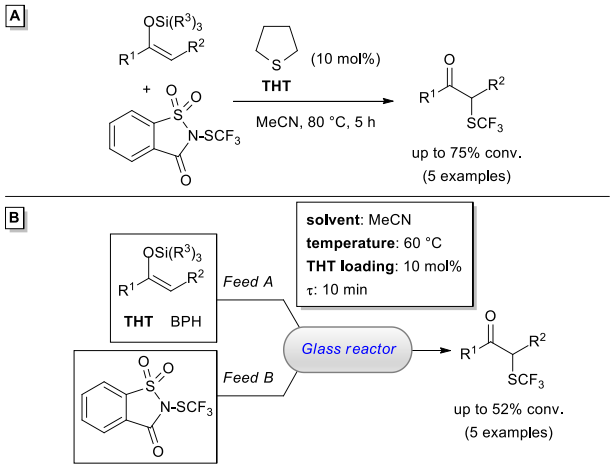

Scheme 5 Organocatalytic α-trifluoromethylthiolation of silylenol ethers. (A) Batch reaction. (B) Reaction in continuous-flow conditions.

From a mechanistic point of view, it has been assumed that the α-trifluoromethylthiolation reaction commences with the activation of the "SCF3" group by interaction of *N*-(trifluoromethylthio)saccharin with THT Lewis base to generate intermediate **5**, in analogy with the sulfenylation of ketone-derived enoxysilanes (Scheme 6).[26] Reaction of **5** with the silylenol ether produces either the silyloxycarbenium ion **6** or the thiiranium ion **7** that are then taken to the final ketone

product through nucleophilic displacement of the silyl moiety by the saccharin counter-ion, concurrently with catalyst release. DFT calculations were run to shed light on the proposed mechanism evidencing that product formation is observed provided that sufficiently high temperature is used.

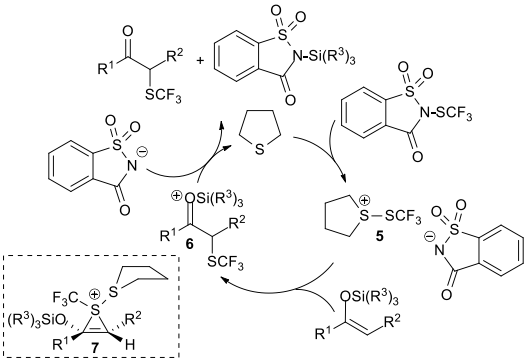

Scheme 6 Proposed catalytic cycle for the α-trifluoromethylthiolation of silylenol ethers.

Recently, Brønsted acid catalysis has shown to be a useful tool for promoting hydrochlorination of biobased glycerol in continuous-flow (Scheme 7).[27]

Among the many tested organic (carboxylic) acids, pimelic acid (10 mol%) gave excellent performances in combination with concentrated aqueous HCl (6 equiv) producing mono- and dichlorohydrins with >99% conversion, 81% cumulated yield and high selectivity for 1,3-dichloro-propan-2-ol (44% yield). The operating conditions called for a reaction temperature of 140 °C and τ = 20 min. The short reaction time represents a crucial feature of this continuous-flow approach, given that a typical batch procedure takes several hours to proceed. In addition, it must be said that aqueous HCl could be used rather than the gaseous one, and a well-documented problem for batch hydrochlorination, namely catalyst evaporation,[28] is prevented by the sealed flow apparatus.

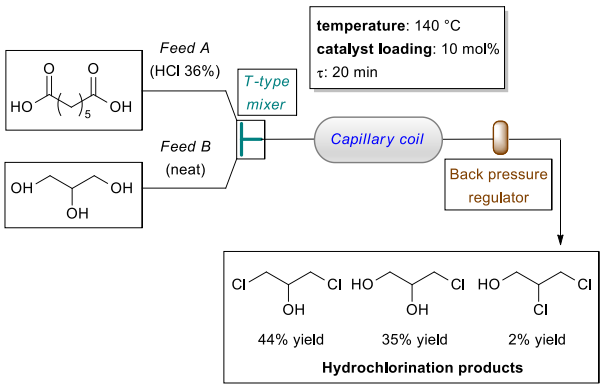

Scheme 7 Continuous-flow hydrochlorination of glycerol catalyzed by pimelic acid.

Tellingly, hydrochlorination of unrefined (biobased crude) glycerol derived from vegetable oils gave very similar results, in spite of the presence of several contaminants: glycerol was quantitatively converted into the corresponding chlorohydrins (61% overall yield) consisting mainly of 3-chloro-1,2-propanediol (41% yield).

Interestingly, glycerol hydrochlorination has been productively concatenated to a dechlorination step under continuous-flow giving access to the oxirane derivatives glycidol and epichlorohydrin (2:3 ratio, 74% cumulated yield), which were separated by an in-line extraction/concentration unit (Scheme 8). The isolated epichlorohydrin was eventually used in further continuous-flow processes to prepare pharmaceutically relevant β-amino alcohols (propranolol, naftopidil, alprenolol) *via* glycidyl ether synthesis followed by aminolysis.

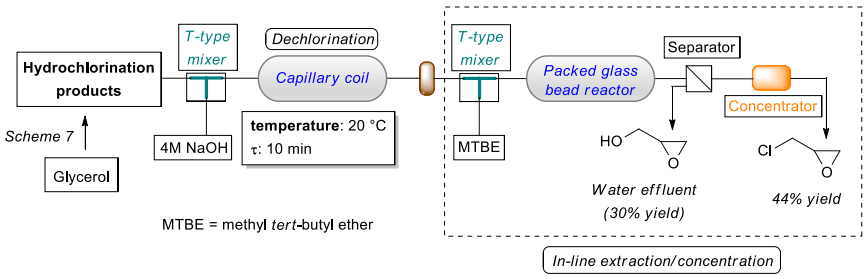

Scheme 8 Transformation of glycerol into oxiranes by a telescoped hydrochlorination/dechlorination process in continuous-flow.

Very interestingly, homogeneous achiral organocatalysis under continuous-flow was brilliantly applied in polymerization reactions.

In this regard, microreactor technology has been investigated for the preparation of polyesters and poly(lactic acid) *via* a ring-opening polymerization (ROP)[29] strategy promoted by 1,5,7-triazabicyclo[4.4.0]dec-5-ene (TBD), which is a robust organocatalyst for ROP of cyclic esters.[30]

In 2016, Zhu *et al.* reported the TBD-catalyzed continuous-flow homopolymerization of δ-valerolactone (VL) and ε-caprolactone (CL) using benzyl alcohol as initiator (100/1/0.5 monomer/alcohol/TBD ratio), by way of a tubular microreactor equipped with a T-type mixer (Scheme 9A).[31]

A mechanism may be postulated according to which TBD plays the role of a bifunctional catalyst (Scheme 9B). Thus, the nitrogen atom of the imine portion attacks the lactone carbonyl group, then proton transfer from the intermediate iminium ion to the incipient alkoxide forms TBD amide **8**. At this point, hydrogen-bond activation of the alcohol initiator promotes esterification freeing the ester and re-creating TBD.[30a]

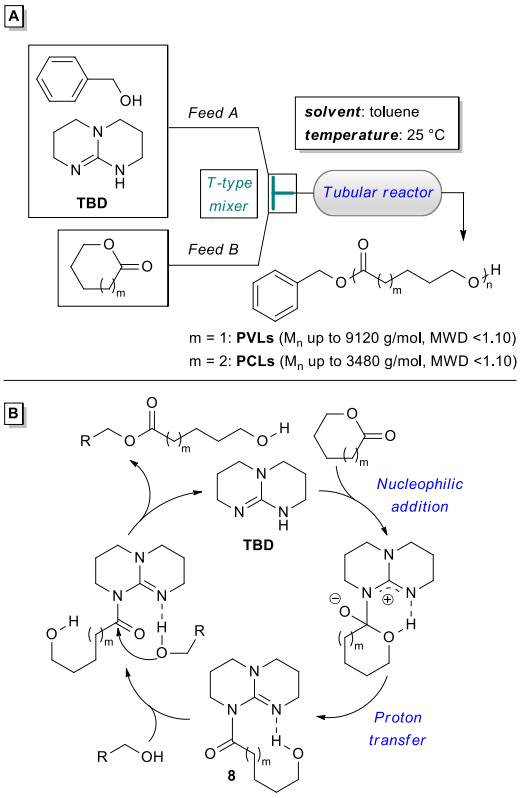

Scheme 9 (A) TBD-promoted homopolymerization of CL and VL under continuous-flow conditions. (B) Possible mechanism.

High-level control of both molecular weight (M_n) and molecular weight distribution (MWD) has been achieved. In particular, M_n values could be efficiently tuned by modulation of FR (hence τ), and specifically the M_n of polymers increased as FR decreased. Thus, polycaprolactones (PCLs) of 2290, 2620 and 3480 g/mol were obtained by applying flow rates of 66, 44 and 33 µL/min (τ = 30, 40 and 60 min, respectively). Similarly, M_n of polyvalerolactones (PVLs) ranged from 2210 to 9120 g/mol as FR went down from 2000 to 133 µL/min over the course of 15 min. Besides, molecular weights showed a very narrow distribution, as demonstrated by MWD of less than 1.10 in each case, indicating that polymerization was living/controlled.

It's important to say that these findings were superior to those obtained in a batch reactor under the same experimental conditions. In the latter case, all polymers showed lower M_n than those prepared by the microreactor approach, maybe because of poorer monomer conversions.

In addition to this, kinetic studies have evidenced that polymerization of VL and CL in microreactor was twice as fast as the analogous batch process. This was assumed to depend on several factors, including more effective reactant mixing, reinforced heat/mass transfer and shorter route for mass transport due to the high surface-to-volume ratio and the microreactor continuous-flow feature.

In parallel, an integrated-microreactor apparatus was developed to achieve efficient block copolymerization of VL and CL by modulated introduction of monomers (Scheme 10). This system led to obtain poly(VL)-*block*-poly(CL) (PVL-b-PCL) and poly(CL)-*block*-poly(VL) (PCL-b-PVL) having a degree of polymerization (DP) of 21 monomer units and a narrow molecular distribution (MWD <1.10). In this case, the polymer which is formed in the first tubular microreactor (τ_1 = 10 min for PVL-b-PCL, τ_1 = 90 min for PCL-b-PVL) acts as the macroinitiator of the subsequent polymerization reaction taking place in the second tubular microreactor (τ_2 = 90 min for PVL-b-PCL, τ_2 = 10 min for PCL-b-PVL) to form the expected block copolymer.

Similarly to homopolymerization, the continuous-flow multiblock copolymerization was more easy and efficient compared to batch processing.

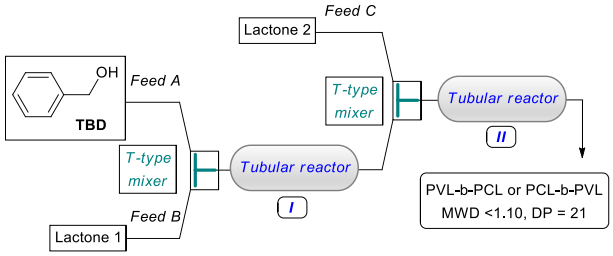

Scheme 10 TBD-catalyzed integrated-microreactor platform for the preparation of PVL-b-PCL and PCL-b-PVL copolymers.

In the same year, TBD catalysis under continuous-flow was exploited by van den Berg *et al.* to obtain well-defined poly(lactic acid) (PLA) by ROP of L-lactide.[32] In this case, polymerization was accompanied by final quenching with benzoic acid in order to suppress concomitant transesterification of the polyester product, which is known to be easily promoted by TBD.[30,33]

As shown in Scheme 11, this study was based on the use of a microreactor apparatus featuring a glass microreactor chip fed with alcohol initiator/catalyst (*Feed A*) and monomer (*Feed B*) solutions. The acid quencher (*Feed C*) was transferred into the reaction stream at the end of the reaction zone thereby precisely controlling the τ value and hence the polymerization process.

Successful reactions have been observed with a wide variety of initiators, such as 4-*tert*-butylbenzyl alcohol, poly(ethylene glycol) (PEG) monomethyl ether as well as bicyclononyne (BCN)- and tetrazine-functionalized alcohols, and suitable conditions were found to be: catalyst loading, 0.25 to 1.2 mol%; reaction temperature, -10 to 30 °C; residence time, 2 to 5 s. As such, the monomer has been turned into polymer products (conversion: 95 to 100%) having polydispersity (PDI) values of ca. 1.2.

Typically, the higher the residence time, the higher the conversion. However, concomitant broadening of MWD was observed as a result of polymer transesterification, in accordance with known data.[30] Meanwhile, appropriate variation of the monomer/initiator ratio allowed to obtain polymers with DP ranging from 80 to 240 (M_n up to 44 000 g/mol).

Importantly, scale-up experiments under the optimized conditions led to obtain more than 120 mg of polymer per hour (93% yield, DP = 76, PDI = 1.19). According to the authors, this result together with the ease of purification (precipitation)

brought the prospect of scaling-up the continuous-flow polymerization at the mesoscale.

It must be said that polymerization in batch mode (0.5 mol% cat., 20 °C, 3 s) followed by manual benzoic acid addition gave lower conversion (49%) compared to an analogous flow experiment (91% conv.), albeit with similar results in terms of PDI (ca. 1.2).

Moreover, the batch reaction needed to be run in a protected environment (glovebox) to keep moisture out, which represented a further major disadvantage over the flow procedure.

Finally, very relevant was the possibility of applying the continuous-flow procedure to the base-labile tetrazine initiator, with no observed degradation that on the contrary rapidly occurs in batch reactions.[34]

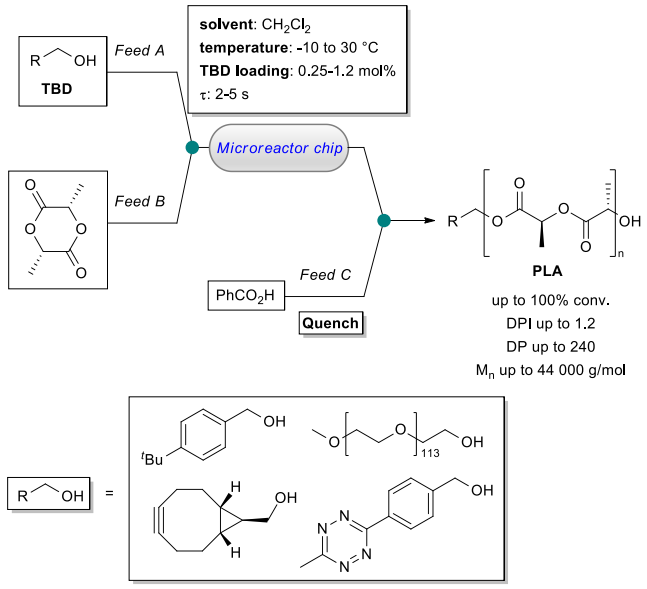

Scheme 11 Continuous-flow synthesis of PLA by TBD-catalyzed ROP.

Interestingly, the BCN-PLA and tetrazine-PLA block copolymers have been further functionalized with either polymers or (bio)molecules *via* strain-promoted azide-alkyne cycloaddition (SPAAC) and inverse electron demand Diels-Alder (IEDDA) click reactions, providing new PLA materials that might find application in biomedicine and beyond.

In 2017, two research teams reported continuous-flow strategies based on organocatalyzed atom transfer radical polymerization (O-ATRP)[35] of methacrylate (MA) monomers and methacrylic acid (MAA) in the presence of an alkyl bromide initiator and a visible-light absorbing photoredox catalyst (PC).

In this respect, Ramsey *et al.* have studied the continuous-flow polymerization of methyl methacrylate (MMA) assisted by *N,N*-diaryl phenazines, perylene and a *N*-aryl phenoxazine (POX) catalyst using either ethyl α-bromophenylacetate (EBPA) or diethyl 2-bromo-2-methylmalonate (DBMM) as the initiators.[36] Extensive experiments demonstrated that DBMM/POX system in *N,N*-dimethylacetamide (DMA) solvent was the best reliable one (Scheme 12A), a monomer/initiator/catalyst ratio of 1000:10:1 being chosen to assure optimum control over the course of polymerization in terms of dispersivity (Đ, 1.25) and initiator efficiency (I*, 95%). This was not the case for high-molecular weight polymers (MMA/DBMM/POX ratio up to 5000:10:1), likely due to the great viscosity of their solutions causing enhanced shear rates inside the reactor and scanty diffusional mixing. As a result, even with unvarying flow rates, polymer chains lengthen and move along the reactor at diverse rates, which leads to a broad distribution of residence times resulting in higher Đ values (up to 1.67) alongside I* superior to 100% (up to 147%).

The continuous-flow O-ATRP methodology was subsequently extended to polymerization of other methacrylate monomers, namely benzyl methacrylate, ethyl methacrylate, poly(2-ethylhexyl methacrylate), lauryl methacrylate, isodecyl methacrylate, and diethylene glycol methyl ether methacrylate. These processes led to polymers with Đ spanning within 1.14 to 1.49 (M_n up to 26.5 kDa), and I* values up to 98% were observed.

In comparison with the O-ATRP batch approach, the continuous-flow method has proven superior, particularly at low monomer conversions. This was evidenced by lower Đ values and increased control over M_n, with almost 100% I*. This outcome has been assumed to depend on the uniform irradiation conditions provided by continuous-flow, resulting in higher concentrations of the PC triplet excited state (^{3}PC*) which is formed in O-ATRP catalytic cycle (Scheme 12B).[37] The ensuing result is a rapid activation of the initiator which indirectly leads to increase the concentration of the deactivator.

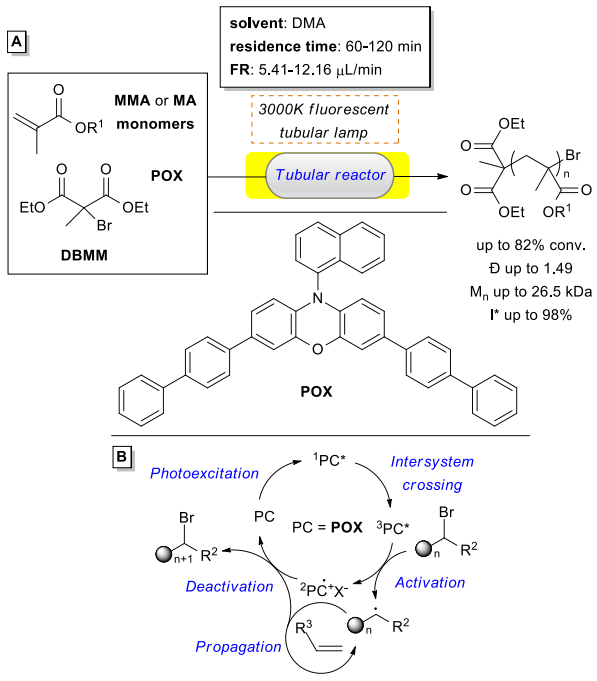

Scheme 12 O-ATRP of MMA and MA monomers in continuous-flow.

Further to this, a PMMA macroinitiator, in turn obtained on large scale (3.3 g, 73% yield), has been fruitfully used as

substrate for chain elongation with isobutyl methacrylate and benzyl methacrylate (Scheme 13).

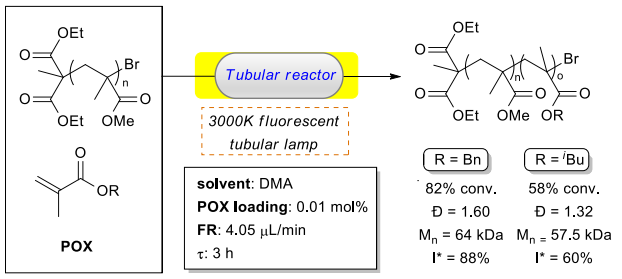

Scheme 13 O-ATRP chain elongation of a PMMA macroinitiator under continuous-flow regime.

A short time later, Ramakers *et al*. described the O-ATRP of MMA and MAA using 10-phenylphenothiazine (PTH) and EBPA as photo-organocatalyst and initiator, respectively (Scheme 14).[38]

In this case, a monomer/initiator/catalyst ratio equal to 100/1/0.05 was applied and flow rates were adjusted in order to obtain reaction times up to 120 min.

Regardless of the monomer substrate, performances were superior to those observed in parallel batch polymerizations, in relation to reaction rate which has been significantly increased. So, the continuous-flow system enabled polymerization of MMA (ca. 50% conv.) in 2 h instead of 12 h, and a similar trend was observed for the synthesis of polymethacrylic acid (PMAA, flow regime: 2 h, 65% conv.; batch reactor: 10 h, 35% conv.).

Still, both batch and flow processes gave low conversions because of the detachment of the bromine terminal moiety from certain polymer chains as a result of bimolecular termination, which supposedly contributed to quite high Đ values (up to 2.2 for MMA polymerization). This unintended issue discouraged further optimization of the flow procedure for the possible purpose of production. Nonetheless, flow conditions were still used to achieve surface grafting of PMAA on silicon wafers.

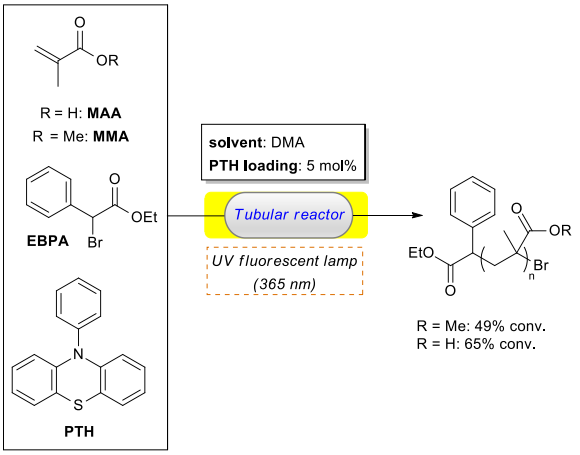

Scheme 14 O-ATRP of MMA and MAA in continuous-flow.

2.2 Homogeneous chiral organocatalysis

Very recent reports concerned the development of continuous-flow transformations catalyzed by homogeneous chiral organocatalysts.

On this issue, Singh's catalyst[39] gave successful results in the asymmetric organocatalytic aldol reaction of a hydrophobic aldehyde (i.e. *m*-chlorobenzaldehyde) with acetone in aqueous medium (Scheme 15).[40]

On the basis of exploratory studies in batch mode (Scheme 15A), this transformation was best run at room temperature in a capillary-type tube reactor for 1 h in 2-propanol/phosphate buffer (pH 7), using 3.6 mol% of the prolineamide organocatalyst (Scheme 15B). Final quench of the reactor effluent with aqueous 2.0 M HCl/CH_2Cl_2 system (1:1 ratio) and typical work-up gave access to the aldol product with 74% conversion and 89% ee.

These results were almost identical and even somewhat better than those obtained in the batch approach (67% conv., 91% ee). With particular regard to conversions, a possible explanation for the different results observed has been proposed basing on the theory of reaction kinetics of ideal plug-flow and stirring-tank reactors operating in continuous and discontinuous mode, respectively. Under homogeneous (ideal) reaction conditions, it is likely that the same conversion is obtained, irrespective of the reactor used, as one could equate a certain volume portion of the plug-flow reaction mixture to a batch reactor volume at the micro-scale.

It also needs to be pointed out that conversion was strictly related to both flow rate and reactor length for the same residence time, indicating that turbulence had a decisive influence over the course of the reaction. This is probably from the hydrodynamic effect (mixing and convection) which makes a substantial contribution to mass transfer under the working flow conditions.

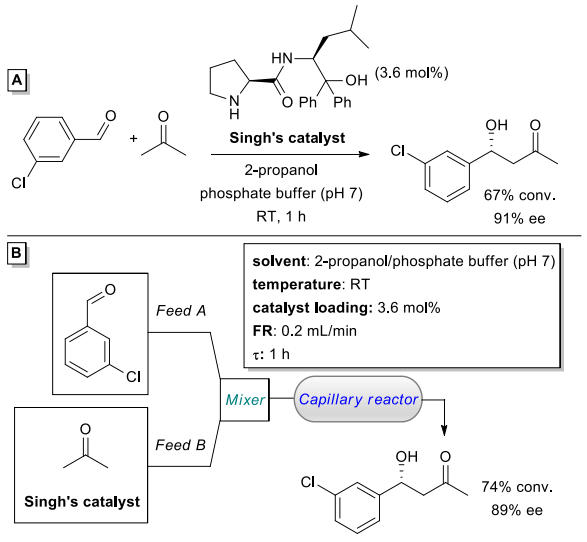

Scheme 15 Asymmetric organocatalytic aldol reaction promoted by Singh's catalyst. (A) Reaction in batch conditions. (B) Reaction in continuous-flow mode.

Robust cinchona-cyclodextrin (CD) organocatalysts featuring thiourea or squaramide core units helped efficaciously in the asymmetric Michael reaction of *trans*-β-nitrostyrene and 1,3-diketones in an integrated synthesis-separation flow process.[41] Preparatory batch operations with both pentane-2,4-dione and diphenylpropane-1,3-dione led to obtain the greatest results (up to 95% yield and 99% ee) from using green solvents, namely 2-methyltetrahydrofuran (MeTHF) and dimethylcarbonate (DMC), as opposed to the traditional ones (toluene, anisole, THF), and, significantly, selectivity was roughly the same for both thiourea and squaramide based catalysts. Analysis in respect of Kamlet-Taft descriptors indicated an inverse relationship between solvent and enantioselectivity, as ee increased with the reducing of the hydrogen-bond donor strength (α) parameter.[42] Notwithstanding, low α values were not sufficient, however necessary, to realize the studied transformations in a highly enantioselective fashion.

In order to trace the road to a continuous catalysis-separation process, a model study was performed using the squaramide-type organocatalyst (5 mol%), diphenylpropane-1,3-dione and the nitroalkene (1.5 equiv) in MeTHF, reactants stoichiometry and catalyst loading being tuned up to completely consume the 1,3-diketone substrate and therefore ease separation (Scheme 16A).

When transferring these optimized conditions from batch to continuous-flow, 100% conversion and 99% ee were attained at 20 °C and at a maximum FR of 4 mL/min.

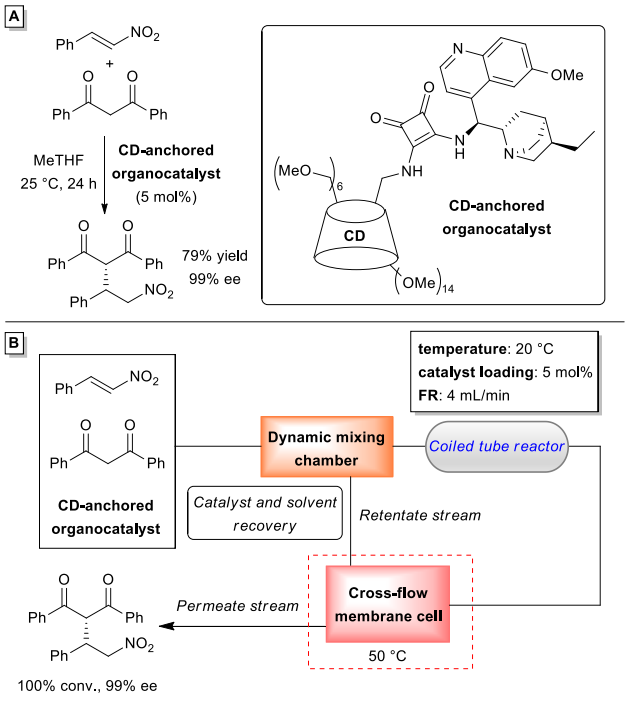

Scheme 16 Michael reaction of *trans*-β-nitrostyrene and 1,3-diketones catalyzed by a CD-anchored cinchona-squaramide organocatalyst. (A) Reaction in batch conditions. (B) Reaction in continuous-flow.

As shown schematically in Scheme 16B, the typical equipment consisted of a coiled tube plug-flow reactor merged with a cross-flow membrane cell (set at 50 °C to prevent product precipitation), which allowed for the separation (*permeate stream*) of the target compound (98% final purity, 99% ee, *P* = 80 g/L h) and the simultaneous recycle (*retentate stream*) of both the catalyst (100%) and the solvent (50%).

With particular focus to the CD-catalyst, it has been shown that both harsh conditions (up to 100 °C) and long-term usage (18 days) had no effect on its sturdiness and reusability. And talking of catalytic activity, it was very likely enhanced due to the anchorage of the cinchona-squaramide residue to CD, resulting in more beneficial interactions (hydrogen-bonds) between the reagents and the catalytic site, as disclosed through *ab initio* calculations.

3. Heterogeneous strategies

3.1 Heterogeneous achiral organocatalysis

In the field of heterogeneous achiral organocatalysis, batch/continuous-flow transformations involving alkynes have been reported by two research groups.

A heterogeneous bifunctional polystyrene (PS) endowed with phenol and phosphine arms (rasta resin) was developed for both batch and continuous-flow organocatalytic synthesis of (*E*,*E*)-dienoates[43] by Trost-Lu isomerization of electron-deficient alkynes (Scheme 17).[44]

After a very thorough investigation of the batch process with respect to some key operational parameters (catalyst loading, temperature, reaction time), it has been found that the rasta resin could operate at 20 mol% loading (80 °C, 24 h, 85% yield, Scheme 17A), and the test isomerization of benzyl hept-2-ynoate to benzyl (2*E*,4*E*)-hepta-2,4-dienoate demonstrated that up to five runs (four reuses) were possible with no catalyst degradation or falloff of activity (80-74% yield range).

Accordingly, a continuous-flow process has been implemented using the rasta resin as the fixed-bed material within a glass rods-based reactor warmed up through an oil bath (Scheme 17B). The outcome of the reaction was highly dependent on both residence time (flow rate) and temperature, and best conditions were found at 100 °C (FR = 0.005 mL/min, τ = 200 min) using toluene as solvent. This provided the utmost conversion (92%), while gradually increasing flow rate (up to 0.05 mL/min), which is to say, decreasing residence time (up to 20 min) made the process less effective (81 to 43% conv.). Similarly, higher temperatures went in parallel with lower yields as a result of resin degradation.

It is worth saying that the reaction could take place even in the absence of the solvent (FR = 0.005 mL/min, τ = 200 min, 86% conv.), which is really important in a perspective of transfer on industrial scale.

Notably, the continuous-flow organocatalytic alkyne isomerization gave shorter reaction times (ca. 3 h) than the batch one (9 h), which may be owed to higher local catalyst concentration in the fixed-bed reactor.

Finally, isomerization of a bit more complicated molecule highlighted the effectiveness of the optimized continuous-flow

method, thus tracing the path to its possible use in the synthesis of natural product intermediates (Scheme 17C).

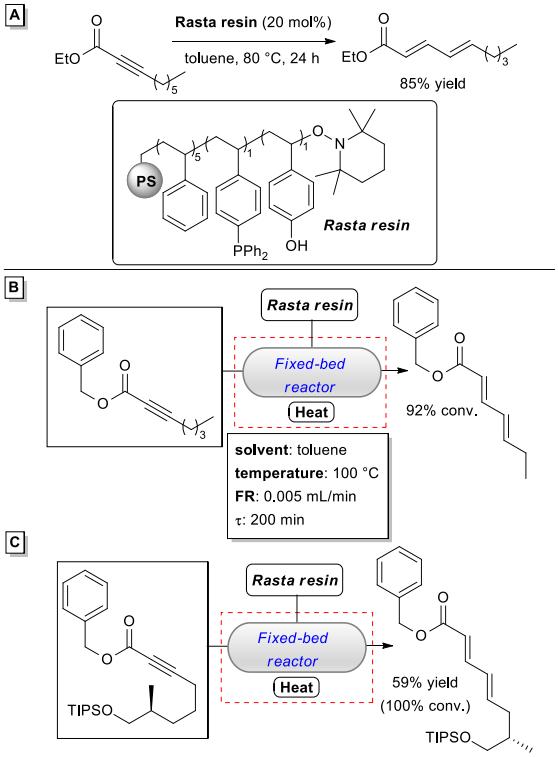

Scheme 17 Trost-Lu isomerization of alkynes catalyzed by rasta resin. (A) Reaction under batch conditions. (B) Reaction in continuous-flow. (C) Application of alkyne isomerization in continuous-flow to the synthesis of natural product precursors.

Recently, triphenyl phosphine-promoted intramolecular α-umpolung Michael addition on activated acetylenes was put in field by Ranjan *et al.* to achieve the synthesis of spiroindolenine derivatives (Scheme 18).[45]

Based on literature data on phosphine-catalyzed annulation of ynones,[46] optimized conditions (20 mol% cat., EtOH, 80 °C, 3 h) were found to establish a wide substrate scope with indole-based propargylic amides, leading to five- and six-membered spiroindolenines with complete *exo*-selectivity (Scheme 18A).

Starting from these results, recyclable polymer-supported triphenylphosphine was prepared and used as heterogeneous organocatalyst for both batch and continuous-flow (packed bed-reactor) spirocyclization of propargylamides (Scheme 18B). A model reaction in batch mode demonstrated that conditions needed to be slightly modified (EtOH, 80 °C, 18 h) and yield was reduced by half (40% *vs* 82%). On the contrary, continuous-flow experiments (EtOH/toluene, 90 °C, FR = 0.025 mL/min, τ = 40 min) gave markedly better results, the test compound being obtained in 88% yield (79% on the gram scale).

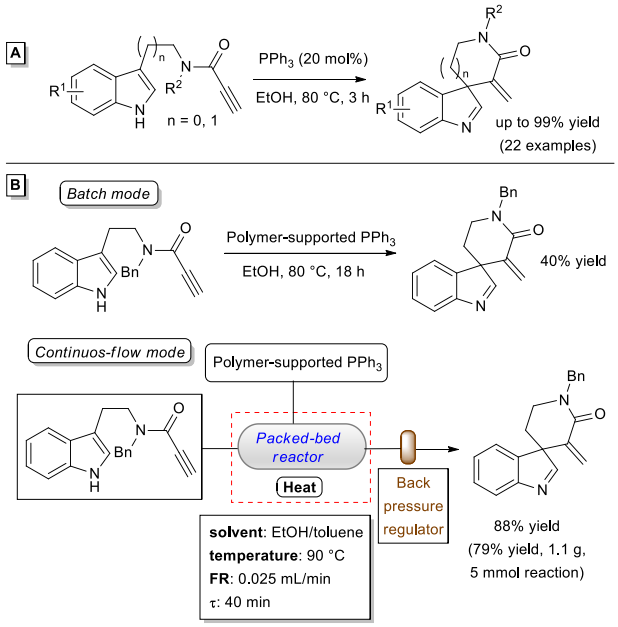

Scheme 18 Synthesis of spiroindolenines by PPh_3-catalyzed α-umpolung Michael addition. (A) Substrate scope for the synthesis of spiroindolenines. (B) Preparation of a model spiroindolenine in batch and continuous-flow conditions with supported PPh_3.

A reasonable mechanism has been postulated also on the basis of ^{31}P NMR experiments. Formation of phosphonium intermediate **9** and its protonation, in sequence, form species **10**. The latter undergoes the decisive α-umpolung addition, then intramolecular proton transfer and phosphine elimination generate the final product (Scheme 19).

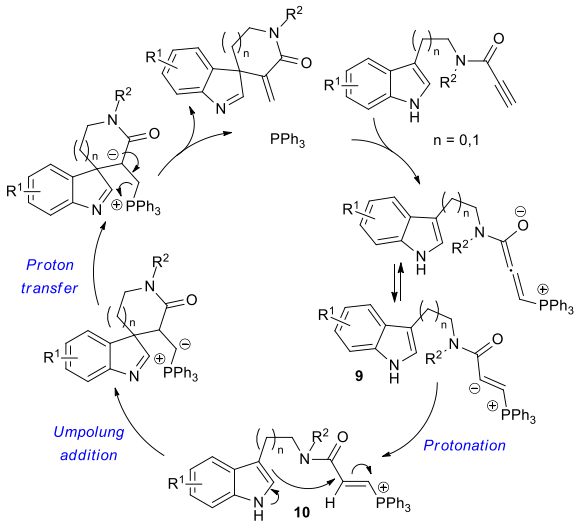

Scheme 19 Proposed catalytic cycle for PPh_3-promoted spiroindolenine formation.

Always within the field of umpolung (polarity reversal) transformations, aroylated α-hydroxy ketones were obtained chemoselectively by benzoin-like reactions of aromatic α-diketones (benzils) catalyzed by commercially available PS-supported 2-*tert*-butylimino-2-diethylamino-1,3-dimethylperhydro-1,3,2-diazaphosphorine (PS-BEMP) (Scheme 20).[47]

Optimal conditions (25 mol% cat., DMF, 50 °C, 16 h) were found for the model cross-benzoin reaction of benzil with *o*-chlorobenzaldehyde in batch (Scheme 20A), which were extended to continuous-flow experiments using a large scope of benzils and aldehyde acceptors (Scheme 20B), the packing bed material showing remarkable long-term stability (ca. 120 h on stream).

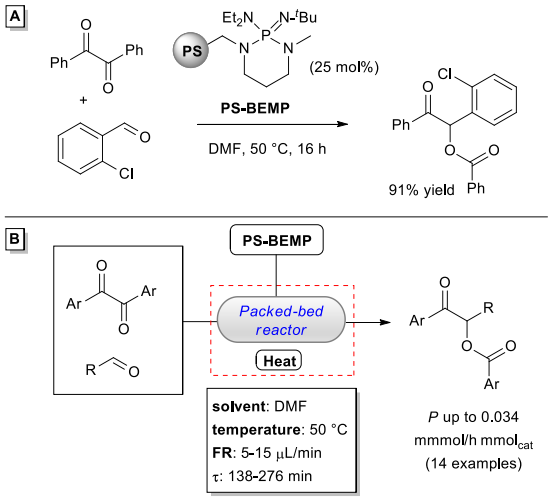

Scheme 20 Benzoin-like reaction promoted by PS-BEMP. (A) Reaction in batch. (B) Reaction in continuous-flow.

In accordance with previous studies on the umpolung reactivity of α-diketones,[48] it is plausible that PS-BEMP deprotonates the DMF solvent generating the carbamoyl anion **11** which then launches two consecutive electron-transfer (ET) processes to the benzil substrate (Scheme 21).

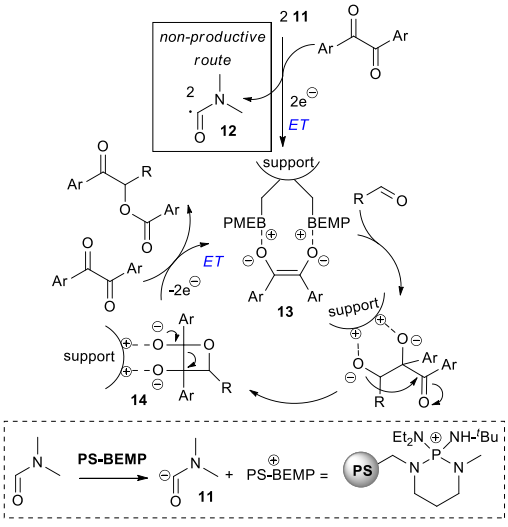

Scheme 21 Proposed mechanism for the formation of aroylated α-hydroxy ketones by PS-BEMP catalysis.

Thus, the carbamoyl radical **12** (*non-productive route*) and the enediolate species **13** are formed, with the latter bound to the polymer as ion pair. Interaction between the heterogenized intermediate **13** and the aldehyde acceptor generates an addition adduct collapsing to the oxetane dianion **14**, which takes part in a conclusive ET giving rise to the final product with concomitant regeneration of enediolate **13**.

It should be emphasized that the polymer support has the great advantage of stabilizing the enediolate moiety thanks to ionic interactions, therefore avoiding its oxidation by air (oxygen) and the subsequent reaction slowdown which have been detected under homogeneous conditions.[48]

Supported NHCs showcased their potential as organocatalysts for carrying out typical transformations in continuous-flow since 2016, when Lupton *et al.* reported the use of a heterogenized imidazolidene catalyst for transesterification of triglycerides.[49] However, the sheer lack of data on the related transformation in batch conditions (catalyst in suspension) makes it difficult to give an objective view on the performances of the continuous-flow process.

In 2018, Ragno *et al.* reported the use of oxidative NHC-catalysis for the preparation of monoacylglycerols (MAGs) by esterification of glycerol and its derivative solketal with aldehydes through the assistance of supported triazolium salt pre-catalysts.[50]

Among different heterogenized NHC precursors, a PS-derived congener appended with a 1-methyl-1*H*-1,2,4-triazole moiety was demonstrated to be the best performing one in batch trials (Scheme 22).

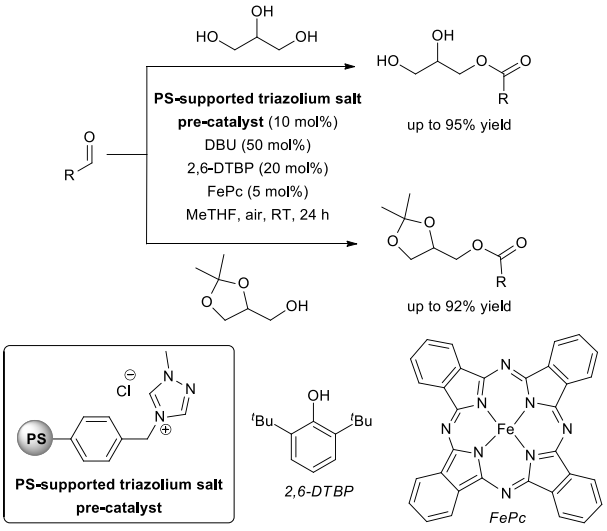

Scheme 22 NHC-catalyzed oxidative esterification of glycerol and solketal in batch mode.

MAGs were produced in high yield (up to 95%) and selectivity (>95:5 monoester/diester ratio) when the heterogeneous triazolium salt pre-catalyst was used at 10 mol% loading in combination with DBU (50 mol%), in the green solvent MeTHF in the presence of the electron transfer mediators 2,6-di-*tert*-butylphenol (2,6-DTBP, 20 mol%) and iron(II) phthalocyanine (FePc, 5 mol%), and air as terminal oxidant.

Equally satisfactory results were found in the exact same conditions starting from the 1,2-isopropylidene derivative of glycerol (solketal) which afforded the corresponding esters in up to 92% yield.

In both cases, the experimental protocol worked well with different types of aldehydes, including aromatic, α,β-unsaturated, long chain aliphatic members as well as the biomass-derived furfural (FF) and 5-hydroxymethylfurfural (HMF), and biogenic vanillin and citronellal.

As represented in Scheme 23, a plausible mechanism for the NHC-mediated oxidative esterification of glycerol and solketal requires that the initially formed Breslow intermediate is engaged in an ET process with the Kharasch oxidant **15**, generated *in situ* from 2,6-DTBP under the basic reaction conditions. Thus, the acyl azolium and the reduced form of the oxidant (**16**) are formed. The former undergoes reaction with the alcohol counterpart to release the anticipated ester, while **16** is re-oxidized by FePc and air (O_2) as the terminal oxidant.[51,52]

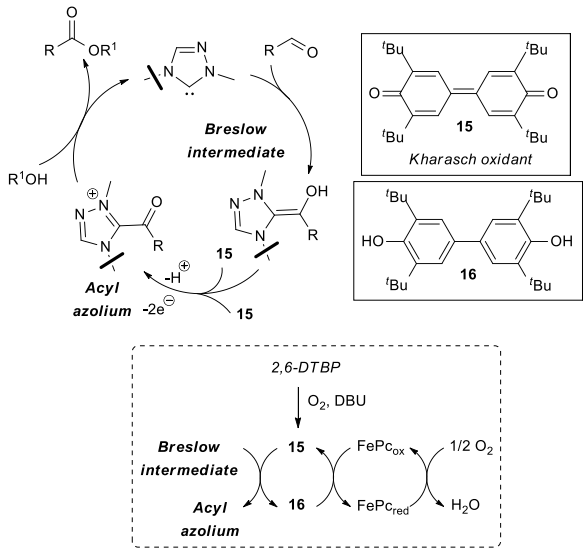

Scheme 23 Proposed organocatalytic cycle for the NHC-oxidative esterification of glycerol and solketal.

The reaction between glycerol and 1-naphtaldehyde was chosen as a testing ground for experiments in continuous-flow using a packed-bed microreactor manufactured with the PS-supported azolium pre-catalyst used for batch tests (Scheme 24).

Presumably due to a low oxygen concentration inside the reactor, the 2,6-DTBP/FePc/air system gave very poor results (15% conv.), while effective outcomes were possible using Kharasch (air-recyclable) oxidant **15**.

Under optimized conditions (50 mol% DBU, 100 mol% oxidant, MeTHF, RT, FR = 35 μL/min, τ = 22 min), the ester product was obtained with total conversion (>95%) and full selectivity (>95%), which were maintained for about 120 h on stream, with an accumulated turnover number (TON) of 71.

The recycled packed pre-catalyst guaranteed 200 h operation, with unchanged selectivity but partial depletion of conversion (45% yield), in analogy to what has been observed in batch (up to ten recycles, preserved selectivity, 5% yield decrease after each recycling, TON_{batch} = 66 with air, 56 with Kharasch oxidant). It is noteworthy that the catalytic activity could not be reestablished despite acidic treatment (37% HCl) to restore the triazolium salt precursor from the *in situ* formed NHC. In the face of this, continuous-flow conditions demonstrated substantial benefit, as productivity (*P* = 0.59 mmol/h $mmol_{cat}$) increased than in batch, thanks to the elimination of contaminants and moisture from the active NHC.[53]

Moreover, continuous-flow conditions could prevent the over esterification of glycerol (at the chosen residence time), provided that it was used in smaller amounts (2 equiv) in comparison to the batch process (3 equiv).

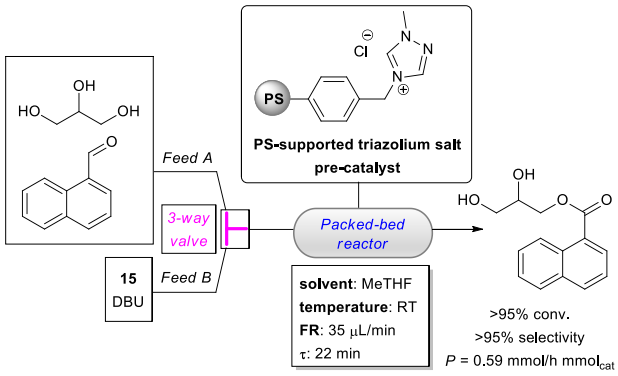

Scheme 24 NHC-induced monoesterification of glycerol under continuous-flow conditions.

In addition, the continuous production of glycerol and solketal esters derived from FF, HMF, vanillin and citronellal was achieved, flow rates (30-35 μL/min) being adjusted in order to obtain conversions higher than 90%. This made simple both product purification and recovery of the reduced form of the oxidant, eventually reoxidized by air (10 mol% FePc, THF, RT). In such a way, the target MAGs were obtained with complete selectivities and good productivities (*P* = 0.5-0.6 mmol/h $mmol_{cat}$).

In the course of studies on the aerobic oxidation of HMF to the corresponding 5-hydroxymethyl-2-furancarboxylic acid (HMFCA) by heterogeneous NHC-catalysis, the effectiveness of the PS-supported triazolylidene catalyst used for the esterification of glycerol (solketal) has been substantiated in the processing of FF and HMF to the corresponding ester, amide, and thioester derivatives (Scheme 25).[54]

In these processes, the optimal catalytic system was represented by a combination of the immobilized triazolium salt pre-catalyst (20 mol%), DBU (50 mol%), FePc (5 mol%) and atmospheric air (terminal oxidant), which gave the targeted compounds in up to 90% yield using a 5-fold excess of nucleophile to limit concurrent HMF polycondensation (Scheme 25A).

The use of FePc as the sole electron transfer mediator originated from parallel studies on the formation of HMFCA and related polyester oligomers (poly-HMFCA) showing that reaction efficiency did not change in the absence of 2,6-DTBP.[54] This means that FePc needs a low energy barrier to mediate the aerobic oxidative esterification of HMF,[55] therefore suppressing the oxygenative route (Scheme 25B, grey pathway) by a faster reaction with the Breslow intermediate than oxygen.

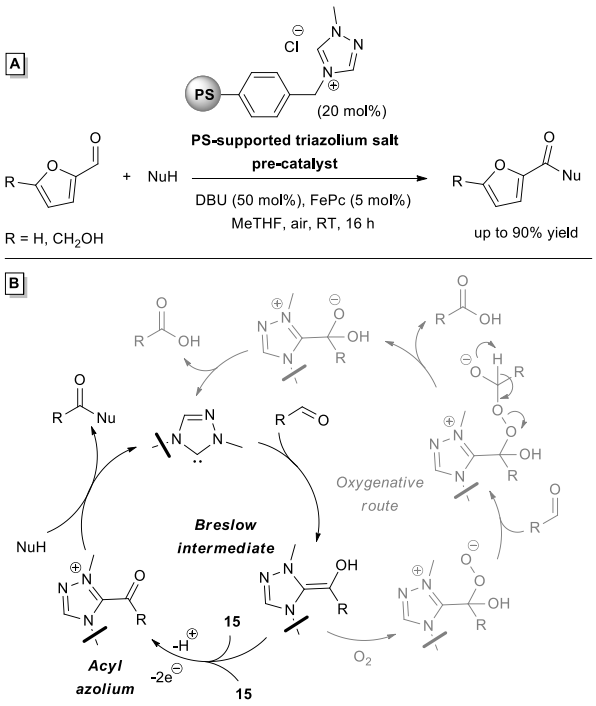

Scheme 25 NHC-promoted aerobic oxidation of FF and HMF. (A) Reaction in batch mode. (B) Organocatalytic cycle and competitive oxygenative pathway.

Next, studies in continuous-flow were conducted as done for glycerol (solketal) esterification.[50] So, a two-pump, three-way valve set-up was used to feed the packed-bed reactor with independent solutions of aldehyde/nucleophile and DBU/Kharasch oxidant **15** (Scheme 26). Here as well, flow rates (30-35 µL/min) were suitably adjusted to get oxidation products of HMF and FF with ≥90% conversion (*P* = 0.46-0.6 mmol/h $mmol_{cat}$), facilitating the work-up of the reactor effluent (product purification and recovery of the reduced oxidant).

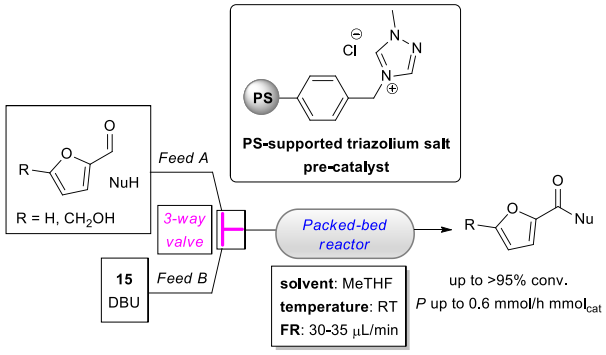

Scheme 26 NHC-promoted aerobic oxidation of FF and HMF under continuous-flow.

As part of a work on the continuous-flow synthesis of chiral cyanohydrins,[56] a two-step process combining organocatalytic cyanosilylation of aldehydes with conversion of the resulting cyanosilyl ethers into the corresponding methyl esters was recently realized by use of supported ionic liquid-like phases (SILLPs) (Scheme 27).[57]

Opening batch studies demonstrated that four different aldehydes were suitable substrates for organocatalyst **SILLP-I** giving excellent yields (up to 99%) of the related cyanosilyl ethers. These were consecutively hydrolyzed and acetylated by **SILLP-II** to generate cyanohydrin methyl esters in 99% yield whatever the aldehyde used. It is worthy of note that all these steps were carried out under solvent-free conditions, with complete atom economy, no waste (i.e. side-products, unreacted materials) formation, and therefore no need for intermediate product purification except filtration.

The cyanohydrin ester derivatives were eventually submitted to enzymatic (Novozym 435) kinetic resolution (KR) to furnish (*S*)-cyanohydrins (>95% ee) and optically pure (*R*)-cyanohydrin acetates (>99% ee).

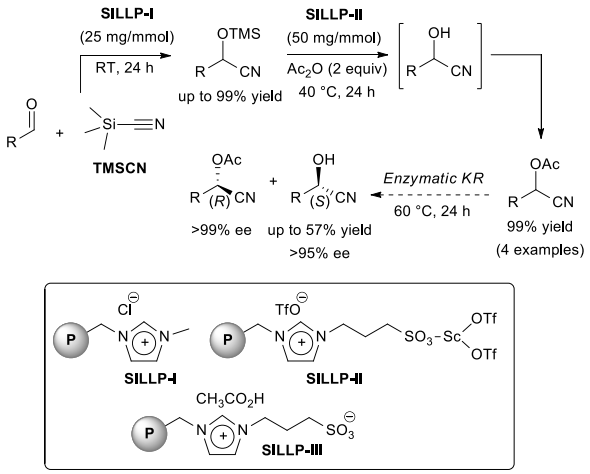

Scheme 27 Synthesis of cyanohydrin acetates by SILLPs catalysis under batch conditions, and possible enzymatic KR.

Unsuccessful attempts to perform the three catalytic steps (cyanosilylation, hydrolysis/acetylation, KR) in a one-pot multicatalytic cascade fashion pushed towards the development of a continuous-flow approach based on the use of consecutive fixed-bed reactors compartmentalizing the different catalytic systems.

For this purpose, synthesis of racemic benzaldehyde cyanohydrin (mandelonitrile) acetate has been investigated as the model process using a system of two in-line reactors packed with organocatalysts **SILLP-I** and **SILLP-II**, respectively (Scheme 28). The first (**SILLP-I**-packed) reactor was fed with neat aldehyde/cyanosilylating agent (TMSCN) mixture and the silyl ether formed was conveyed to the second reactor (**SILLP-II**-packed), simultaneously receiving a stream of acetic anhydride (2 equiv).

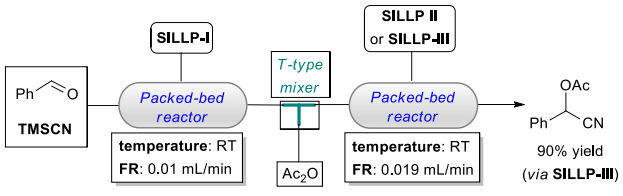

Scheme 28 Telescoped continuous-flow process for the preparation of cyanohydrin acetates.

Unluckily, the poor long-term stability of **SILLP-II** on stream (24 h) compared to **SILLP-I** (50 h) precluded any possible use of this system for continuous production of the target compound, since the cyanosilyl ether was detected as the prevalent product at the exit of the second reactor.

Importantly, this problem has been well overcome by replacing **SILLP-II** with the bifunctional **SILLP-III** catalyst, displaying a uniform catalytic activity over a period of more than 40 h, with a ca. 90% stable yield for mandelonitrile acetate.

Productivity for each step ranged from 100 to 200 mg/h g and very low E factor (waste-to-product ratio) values for both the cyanosilylation step (E = 0.1) and its combination with the hydrolysis/acetylation one (E = 0.93) were observed, evidencing the green features of the combined continuous-flow processes. Eventually, the KR step could be pursued by an in-line added third reactor fixed with the enzyme promoter (Novozym 435), giving rise to (*R*)-mandelonitrile acetate in >99% ee (50 % conv., not shown).

A mechanistic model for the formation of mandelonitrile acetate by consecutive catalysis of **SILLP-I** and **SILLP-III** is highlighted in Scheme 29.

Electrophilic activation of the aldehyde starting material by the C-2 imidazolium hydrogen of **SILLP-I** may be evoked as the key step towards the formation of the cyanosilyl ether. At this stage, **SILLP-III** intervenes by an "electrophile-nucleophile dual activation", thanks to the contemporary presence of acidic and basic sites which operate through a network of cooperative hydrogen-bonds[58] both in the formation of cyanohydrin and in its esterification.

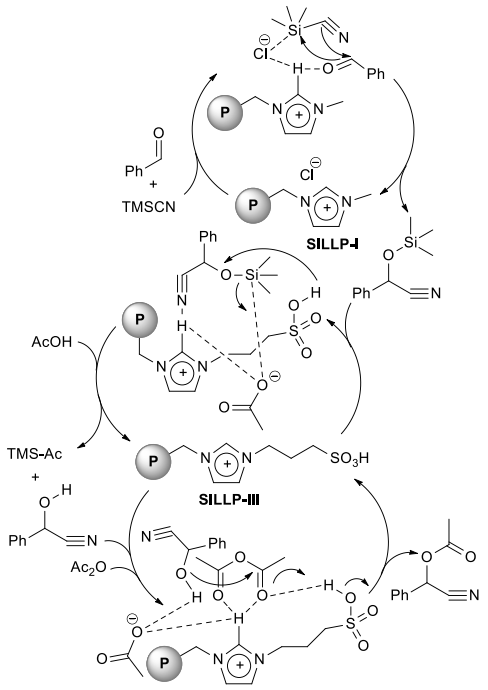

Scheme 29 Postulated mechanism for the formation of mandelonitrile acetate by consecutive catalysis of **SILLP-I** and **SILLP-III**.

3.2 Heterogeneous chiral organocatalysis

Several examples have been found in the literature of the years 2016-2019 relying on the use of differently supported chiral organocatalysts with various activation modes.

In this context, immobilization of 2,4,6-tris-isopropyl BINOL-derived phosphoric acid (TRIP)[59] onto PS resulted in the heterogeneous Brønsted acid organocatalyst PS-TRIP,[60] which was tested in asymmetric aldehyde allylboration (Scheme 30).[61]

It has been shown that highly enantioenriched homoallylic alcohols (up to 96% ee) could be obtained in batch from a wide range of aldehyde starting materials and allylboronic pinacol ester (Scheme 30A) under fine-tuned reaction parameters (5 mol% cat., toluene, -30 °C, 6 h).

It is certainly remarkable that the same sample of PS-TRIP has been used profusely to run all the aldehyde scope (18 examples) without observing a decrease in activity, except when a pyridine substituted substrate has been used. Despite this, the catalytic activity could be restored completely by a simple acidic washing (HCl in EtOAc). Overall, this demonstrated the unique robustness of PS-TRIP, also supported by an accumulated TON_{batch} value of 321.

Apart from this, excellent results have occurred in dimethylallylation (93% ee) and *trans*-crotylation (95:5 dr, 98% ee) of benzaldehyde, while *cis*-crotylation gave lower enantioselectivity (83% ee), maybe because of a competitive background process.

The related flow process has been successfully tested over the reaction between benzaldehyde and allylboronic pinacol ester (Scheme 30B). The device used (three-pump system) incorporated a reactor packed with PS-TRIP, fed with the two reactant solutions, and any unreacted aldehyde was scavenged downstream by aqueous $NaHSO_3$ solution. This was necessary to avoid reaction between excess allylboronic ester and residual aldehyde in the collection flask, thereby preserving product enantioselectivity.

After 28 h operation time (25 °C), the expected product was obtained with yield (92%) and enantioselectivity (91% ee) only slightly lower than those observed in the batch process (96% yield, 95% ee). The total TON_{flow} was equal to 282, *P* amounted to 2.22 mmol/h g_{resin} and no appreciable decay of catalyst activity was detected throughout the experiment.

It can be remarked that all these results, together with the ease of PS-TRIP reactivation, revealed the possibility of extending the flow procedure to large scale production of the enantiopure homoallylic alcohol with very low energy and material costs, as well as in short times.

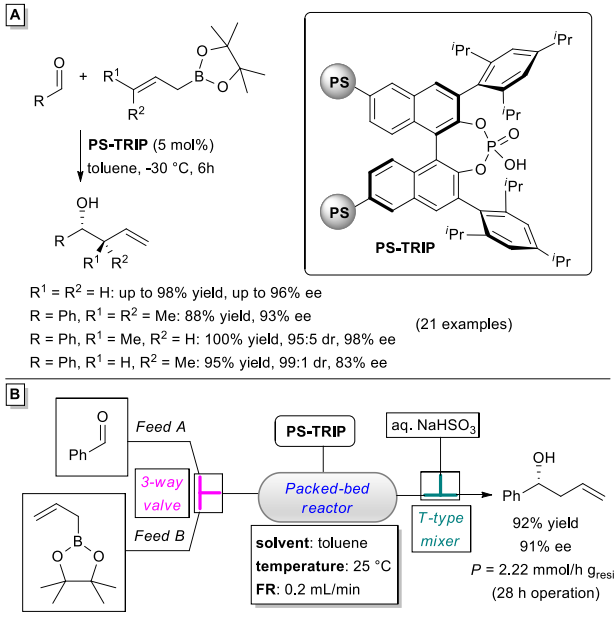

Scheme 30 Asymmetric allylboration of aldehydes catalyzed by PS-TRIP. (A) Batch process. (B) Enantioselective allylboration of benzaldehyde in continuous-flow.

Heterogenized chiral amines (enamine/iminium ion activation) have been the subject of intense research in the field of continuous-flow transformations.

Cañellas *et al.* took advantage of a PS-supported chiral vicinal diamine (triflate salt) to accomplish the enantioselective synthesis of chiral bicyclic diketone compounds *via* Robinson annulation (Scheme 31).[62]

High-throughput experimentation (HTE) in batch mode brought to identify the best conditions (10 mol% cat., 10 mol% TfOH, 5 mol% *m*-$NO_2C_6H_4CO_2H$, 55 °C, MeTHF) for obtaining Wieland-Miescher (W-M) and Hajos-Parrish (H-P) ketones[63] and their analogues (up to 90% yield and 97% ee) from cyclic 1,3-diketones and vinyl ketones (Scheme 31A). Remarkably, shorter reaction times (up to 12 h) were observed than in known procedures (1-7 days) carried out with structurally related homogeneous organocatalysts.[64]

With specific reference to the preparation of W-M ketone, the heterogeneous diamine promoter has proven to be recyclable for just three times owing to significant drop in yield (1st cycle: 98%, 3rd cycle: 65%), probably due to the collateral formation of aza-Michael adducts between amine catalyst and methyl vinyl ketone. This disturbing process could be eluded using a suitable *meso*-triketone as the starting material (Scheme 31B), allowing the catalyst to be re-used in ten sequential cycles (10th cycle: 80% yield, 92% ee).

Based on these results, the asymmetric synthesis of W-M and H-P ketones in continuous-flow was designed using the set up drawn in Scheme 31C, MeTHF being replaced by DMF to bypass solubility problems.

A medium pressure liquid chromatography (MPLC) jacketed glass column was packed with the PS-diamine catalyst (in the form of triflate salt) and fed with both the acid additive and a solution of the triketone precursor, in turn arising from a batch reaction between cyclic 1,3-diketone and vinyl ketone substrates (DMF, 60 °C, 4 h, 100% conv.) in the presence of PS-supported DBU (2 mol%). This has kept the Michael acceptor from entering the reactor avoiding therefore deactivation of the heterogenized organocatalyst by the competitive aza-Michael reaction.

In this way, enantioenriched W-M ketone (91% ee) was prepared on a scale of 65.5 mmol (11.7 g) in a 24 h operation time, which corresponded to an outstanding TON_{flow} of 117. Similarly, seven additional Robinson annulation products were obtained, turnover frequency (TOF) values ranging from 6.7 to 9.3 mmol/h $mmol_{resin}$ as proof of very high productivity. Furthermore, enantioselectivity was comparable to that recorded in batch experiments (78-94% ee *vs* 80-93% ee).

Last, but not least, the heterogeneous organocatalyst has shown considerable robustness, as the preparation of W-M ketone gave very similar results to those obtained in the 24 h experiment in flow even after seven sequential runs with diverse substrates.

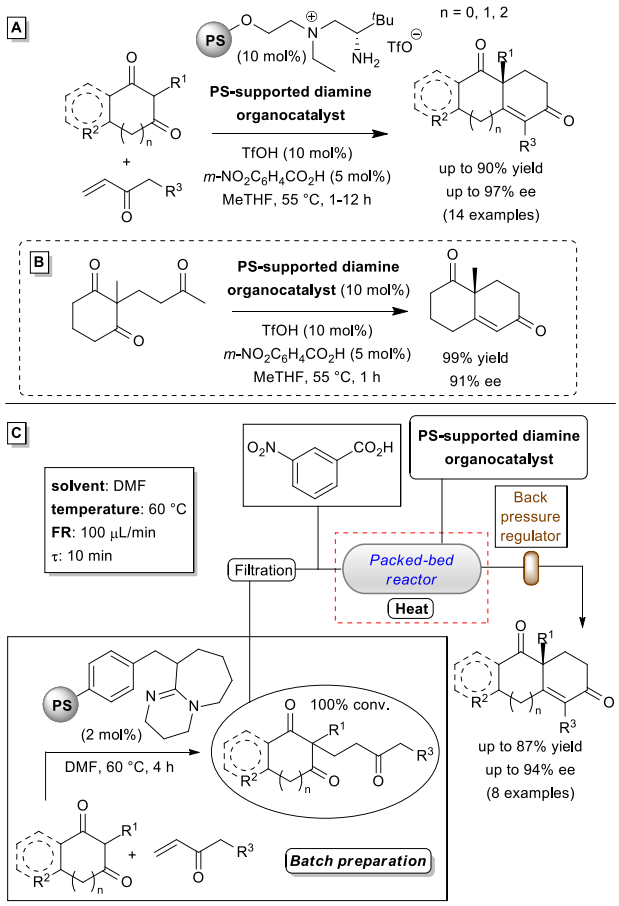

Scheme 31 Robinson annulation reactions promoted by a PS-supported diamine organocatalyst. (A) Reactions in batch mode. (B) Reactions in continuous-flow.

In 2016, Ley-Arvidsson-Yamamoto (*S*)-5-(pyrrolidin-2-yl)-1*H*-tetrazole (here abbreviated as L-A-Y) catalyst[65] has been formulated by Greco *et al.* as a polystyrene monolith to promote asymmetric cross aldol reaction in the green water-ethanol solvent.[66]

Beginning batch experiments on the model reaction between cyclohexanone and *p*-nitrobenzaldehyde have brought to obtain the desired aldol product (90% ee_{anti}, 5:1 dr *anti*/*syn*) in

1:1 water-ethanol at room temperature (Scheme 32), higher temperatures (50 °C) putting down enantioselection (82% ee_{anti}), contrary to known data showing the favorable effect of heating on the activity of both homogeneous and silica-supported pyrrolidinyl-tetrazole catalysts.[67]

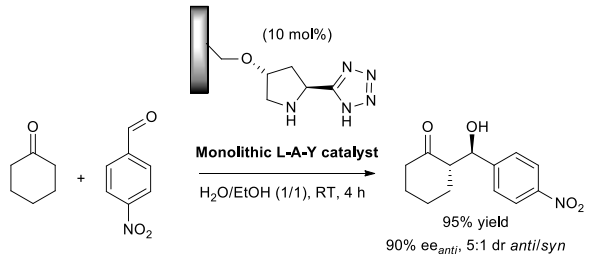

Scheme 32 Asymmetric aldol reaction promoted by monolithic L-A-Y catalyst in batch mode.

It has been demonstrated that the monolith L-A-Y catalyst could be recycled up to eight times ensuring nearly constant yield (95%, TON_{batch} = 80) and only modest decreased stereoselectivity (5:1 dr *anti*/*syn*, 88% ee_{anti}) after the 8th cycle. With these results, a continuous-flow setup has been developed using a suitably assembled monolithic microreactor based on the L-A-Y catalyst (Scheme 33). Under optimized conditions (5 h, 25 °C, 1:1.5 H_2O/EtOH, FR = 20 µL/min, τ = 65 min), the predicted β-hydroxyketone was obtained with little bit better diastereoselectivity (7:1 dr *anti*/*syn*) than in batch reaction, and unaltered enantioselectivity (90% ee_{anti}).

A noticeable thing is that the flow procedure has been enhanced with on-line flow-injection analysis to run the reaction (Scheme 33A, ***D**irection I*, green color) and monitor its progress (Scheme 33A, ***D**irection II,* orange color) at once. That has been possible through the use of a 6-port 2-position (6p 2p) switching valve as the key component of the 2**D** system. This device served to flush the effluent from the reactor into a chiral HPLC column with diode-array detection (DAD), in turn supplied with hexane/^{i}PrOH solvent mixture through the same 6p 2p valve. The conceived 2**D** setup turned out to be a very important tool for studying the batch-to-flow transition of the model reaction between cyclohexanone and *p*-nitrobenzaldehyde, different substrate concentrations and flow rates being evaluated.

Speaking of the stability of the monolithic column under flow regime, it was found that both stereoselectivity and steady-state conversion remained the same for approx. 120 h operation (TON_{flow} = 147). After this time, efficiency decreased gradually, especially in stereoselectivity, probably because of accumulation of impurities onto the monolithic catalyst.

According to these results, continuous-flow aldol reactions of several activated aromatic aldehydes with cyclopentanone and cyclohexanone (FR = 15-20 µL/min) were carried out providing the corresponding aldol adducts in generally good enantioselectivity (up to 95% ee_{anti}), diastereoselectivity closely depending on ketone type (cyclopentanone: up to 2:1 dr, cyclohexanone: up to 7:1 dr) (Scheme 33B).

Identical conditions except temperature (0 °C) and flow rate (10-15 µL/min) were adopted to react acetone in water medium (1.5:1 H_2O/acetone) and obtain the expected β-hydroxyketones with acceptable enantioselectivities (71-88% ee) (Scheme 33B). In all cases, productivity (*P* = 0.61-1.22 mmol/h $mmol_{cat}$) was about twice that observed in batch conditions.

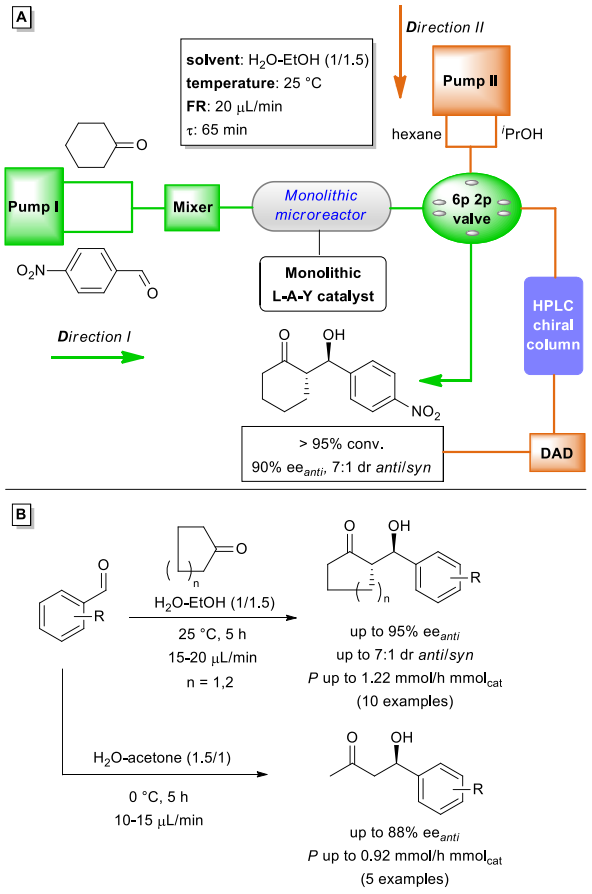

Scheme 33 (A) 2**D** setup for flow aldol reaction and on-line flow-injection analysis. (B) Continuous-flow aldol reactions of aromatic aldehydes with cyclic ketones and acetone.

Interestingly, two years later Nakashima and Yamamoto reported a very unconventional strategy for heterogeneous organocatalysis under continuous-flow relying on the use of a bed-type column packed with an excess of unimmobilized L-A-Y catalyst (Scheme 34).[68] The latter functioned as a heterogeneous organocatalyst when using low-polarity organic solvents which did not dissolve it, while solubilizing substrates and products throughout the course of the reaction.

Hence, cross aldol reactions between acetone and arylaldehydes were effectually executed with the proline tetrazole packed-bed system using a solvent combination of EtOAc (10 vol%) and H_2O (3 mol%) at room temperature (Scheme 34A). These processes provided aldol products in up to >99% yield with fair to excellent enantioselectivities (62-97% ee), the effect of added H_2O resembling that already documented for batch approach.[65a]

And very remarkably is the fact that yields for the reactions of *p*-bromobenzaldehyde (>99%) and *o*-chlorobenzaldehyde (>99%) have been increased by over 15% compared to the related batch transformations.[65a]

Mechanistically, it may be assumed that dissolved proline tetrazole participates in a typical catalytic cycle involving enamine **17** and iminium ion **18** as the key species, the latter undergoing hydrolysis to release the aldol product with concomitant catalyst regeneration (Scheme 34B).

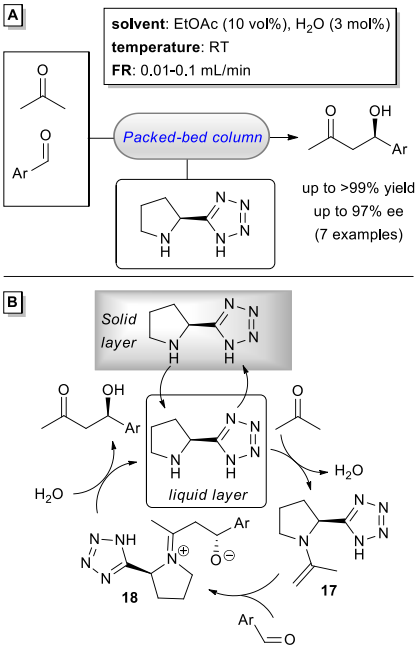

Scheme 34 Aldol reactions of acetone and arylaldehydes using proline tetrazole packed-bed reactor. (A) Continuous-flow process. (B) Proposed mechanistic pathway.

Particularly noteworthy is that the proline tetrazole-based flow column could be operated up to ten times for the reaction between acetone and 2,6-dichlorobenzaldehyde (9.9 mmol scale) without loss of catalyst activity (93% yield, 97% ee).

Moreover, scale-up of the aldol process involving acetone and *p*-nitrobenzaldehyde (52 mmol scale) was possible using a catalyst quantity ten times bigger, producing the expected final compound in 94% yield and 72% ee (24 h, FR = 0.366 mL/min).

Noticeably, the effectiveness of the proline tetrazole packed-bed flow reactor has been further confirmed in aldol, Mannich and *o*-nitroso aldol reactions of cyclohexanone (MeCN or DMF, RT, FR = 0.03 mL/min) giving products in excellent stereo- and chemoselectivity (Scheme 35).

It may be of interest to point out that the authors introduced a new metric, namely process catalyst mass efficiency (PCME), to estimate the efficiency of an organocatalyst subjected to continuous (repeated) use for heterogeneous flow synthesis through packed-bed columns, other typical parameters (e.g. atom economy and E factor) not being particularly suitable for this purpose. In detail, PCME represents the precise amount (measured in mg) of *i)* heterogenized catalyst used or *ii)* non-supported organocatalyst consumed relative to the quantity (mmol) of the targeted product.

In this regard, it was demonstrated that the non-supported proline tetrazole catalyst gave a PCME value of 0.01, which was extremely low compared to diverse polymer- and silica-supported organocatalysts (PCME = 7.6-377.4).

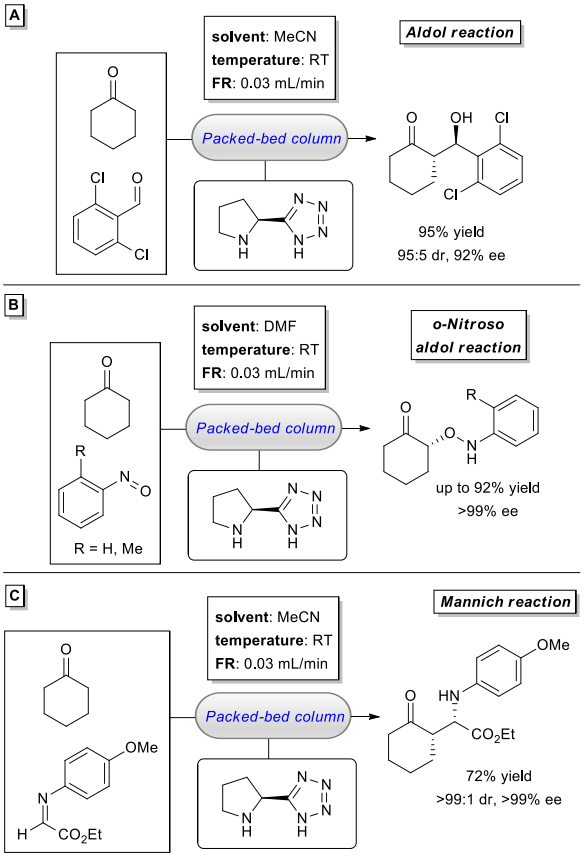

Scheme 35 Application of proline tetrazole packed-bed reactor in aldol, Mannich and *o*-nitroso aldol reactions of cyclohexanone under continuous-flow.

Hayashi-Jorgensen (here abbreviated as H-J) catalysts[69] grafted onto PS through benzyl and 1,2,3-triazole-type linkers have been used for heterogeneous organocatalytic reactions in both batch and continuous-flow conditions, too.

In 2016, immobilized *tert*-butyldimethylsilyl (TBS)-protected *trans*-4-hydroxydiphenylprolinol (**HJ-I**, benzyl linker) has been applied to the enantioselective cyclopropanation of α,β-unsaturated aldehydes with dimethyl bromomalonate (Scheme 36).[70]

Preliminary inspection of the batch reaction (Scheme 36A) enabled the identification of optimal reaction conditions (10 mol% cat., *N*-methylimidazole, CH_2Cl_2, RT, 1 h) to be transferred to the flow method, and accordingly, a library of 12 cyclopropane derivatives was prepared using the device schematically represented in Scheme 36B.

Excellent stereoselectivities (up to 96% ee, >95:5 dr) were detected after 6 h running at 100 µL/min, *P* reached values of up to 2.1 mmol/h g_{resin}, and the supported organocatalyst proved to be particularly robust (total TON_{flow} = 94, up to 76 h operation).

By-product formation *via* secondary transformations (i.e. cyclopropane ring-opening) was decisely minimized compared to both batch (with **HJ-I**) and homogeneous (with

unimmobilized catalyst) experiments. This was possible in virtue of a shorter contact time between the catalyst/base and the final product (especially in the case of electron-rich aldehydes), thanks to the use of an in-line liquid/liquid separator removing base from the effluent flow.

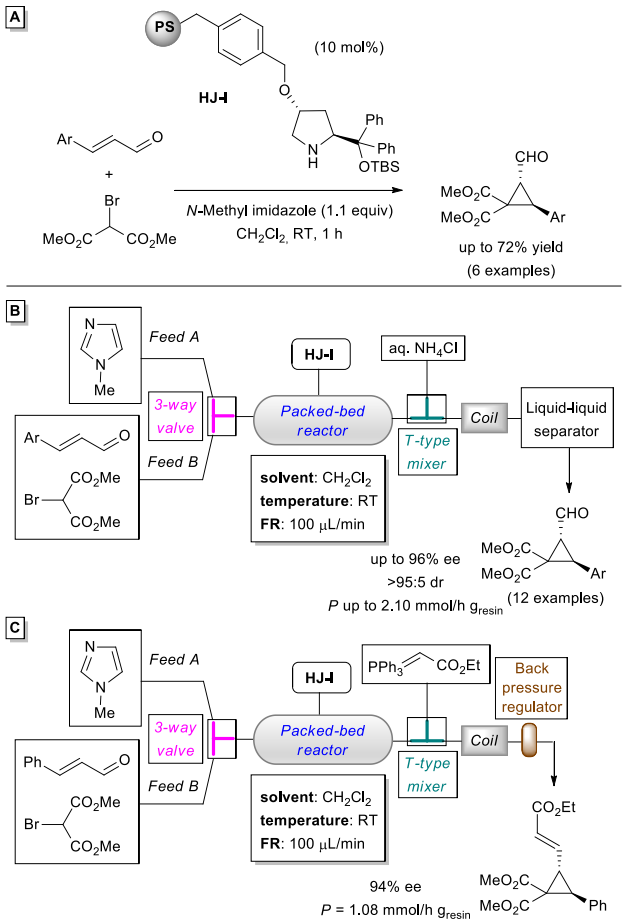

Scheme 36 Organocatalytic cyclopropanation of α,β-enals promoted by PS-supported diphenylprolinol catalyst (**HJ-I**). (A) Reaction in batch conditions. (B) Reaction in continuous-flow. (C) Telescoped cyclopropanation-Wittig reaction in continuous-flow.

It matters to highlight that a reactor packed with the **HJ-I** catalyst could be used intermittently for one year without observing loss of activity.

It is also the case that further molecular complexity has been generated by telescoping the cyclopropanation step with a Wittig reaction, the reactor effluent being fed with a Wittig ylide (Scheme 36C).

The synthesis of 5-hydroxyisoxazolidines by tandem aza-Michael/hemiacetalization reaction between α,β-enals and *N*-protected hydroxylamines was effectively promoted by a PS-supported TBS-protected *cis*-4-hydroxydiphenylprolinol organocatalyst bearing a 1,2,3-triazole spacer (**HJ-II**) (Scheme 37).[71]

Initial evidences in batch offered guidance on the best experimental conditions and reaction scope providing the target products in moderate to good yields (34-83% yield) with good to high enantioselectivities (71-99% ee) and complete diastereoselection (Scheme 37A). After that, it has been seen that the reaction can be run ten consecutive times with the same sample of catalyst without worsening yield and enantioselectivity, so much so that the results recorded in the initial cycle matched those observed in the 10th one (total TON_{batch} = 36.5)

Based on this, next experiments in continuous-flow proceeded smoothly to give 5-hydroxyisoxazolidines with up to 67% yield and up to 99% ee (Scheme 37B). These processes gave an accumulated TON_{flow} value of 134, and it was possible to use the same packed-bed reactor for 2 months without detecting performance losses.

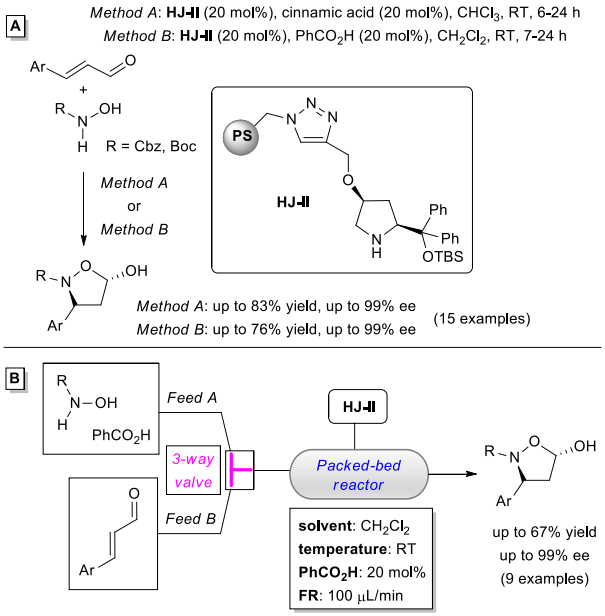

Scheme 37 Organocatalytic synthesis of 5-hydroxyisoxazolidines catalyzed by PS-supported diphenylprolinol catalyst (**HJ-II**). (A) Reaction in batch conditions. (B) Reaction in continuous-flow.

The **HJ-II** catalyst as well as a Wang resin-supported analogue have been used in asymmetric Michael addition reactions to provide pivotal chiral intermediates for the important serotonin reuptake inhibitors (-)-paroxetine,[72] (+)-paroxetine and (+)-femoxetine.[73]

Specifically, Ötvös *et al*. have investigated the **HJ-II** promoted conjugate addition of dimethylmalonate to *p*-fluorocinnamaldehyde,[72] proving that optimum batch conditions (20 mol% cat., 0.6 equiv AcOH, 25 °C, CH_2Cl_2, 24 h, 69% conv., 98% ee, Scheme 38A) could be easily adapted to the continuous-flow regime (FR = 100 μL/min, τ = 35 min) to get identical enantioselectivity, though with a pretty poor (20%) conversion. However, the latter could be increased by enhancing temperature (50 °C, 68% conv.) and malonate concentration (15 equiv, 64% conv.), enantiocontrol remaining unchanged (up to 99% ee).

This important achievement paved the way to further implementation of the flow process in the absence of solvent (Scheme 38B). In this case, very good conversion (93%) and enantioselection (97% ee) were obtained using 2 equiv of malonate at 60 °C (FR = 70 μL/min, τ = 20 min) and importantly,

these conditions have been successful in a 7 h preparative scale experiment giving the target product in 97% ee with a distinguished productivity of 2.47 g/h (17.26 g, 84% isolated yield) and minimal formation of waste (E factor = 0.7).

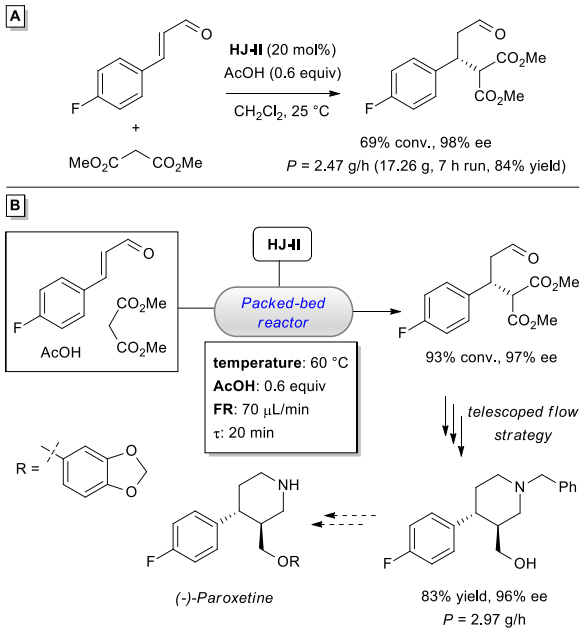

Scheme 38 Organocatalytic asymmetric Michael reaction of *p*-fluorocinnamaldehyde and dimethyl malonate promoted by **HJ-II** catalyst. (A) Reaction in batch conditions. (B) Reaction in continuous-flow under solvent-free conditions.

It should be emphasized that despite the solvent-free conditions, selectivity of **HJ-II** was constant throughout the long-term test (100% chemoselectivity, 95-98% ee) and catalytic activity has suffered a very small decrease (93-85% conv.), validating catalyst robustness.

Overall, these data resulted in an effective catalyst loading of 0.6 mol%, while TON_{flow} and STY values were 132 and 1.76 kg/L h, each in order.

The chiral aldehyde thus obtained underwent a telescoped flow synthesis procedure (not shown) based on a reductive amination/lactamization/amide-ester reduction sequence to produce eventually a key chiral piperidine precursor of (-)-paroxetine.

A Wang resin-immobilized *trans*-4-hydroxydiphenylprolinol organocatalyst (**HJ-III**, triazole linker) has been applied by Szcześniak *et al*. in Michael reactions between aldehydes and *trans*-nitroalkenes to obtain chiral γ-nitroaldehydes, precursors to (+)-paroxetine and (+)-femoxetine (Scheme 39).[73]

Supported by the outset results in batch (15 mol% cat., 20 mol% $PhCO_2H$, $CDCl_3$, RT, 4-5 h, 100% conv., up to 4.6:1 dr *syn/anti*, up to 93% ee_{syn}) shown in Scheme 39A, very diverse reaction conditions have been tested for the continuous-flow asymmetric conjugate addition, with special attention given to the optimization of flow rate to achieve quantitative conversion with no isomerization. Results were best with FR = 5 μL/min, yielding the anticipated γ-nitroaldehydes in up to 3.8:1 dr *syn/anti*, which is a bit worse than in the batch process (Scheme 39B). On the contrary, the observed ee was like that for the batch strategy whichever procedure was used.

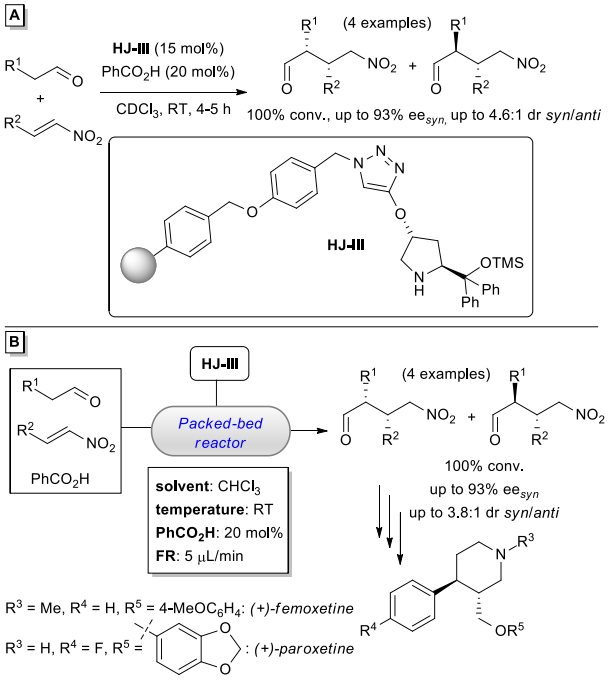

Scheme 39 Organocatalytic asymmetric Michael reaction between aldehydes and *trans*-nitroalkenes promoted by Wang resin-supported diphenylprolinol catalyst (**HJ-III**). (A) Reaction in batch conditions. (B) Reaction under continuous-flow conditions.

Interestingly, silica-supported L-A-Y and H-J catalysts have been exploited for heterogeneous enantioselective organocatalysis at the microscale through a lab-on-a-chip approach,[74] based on the use of a miniaturized microfluidic chip integrating a packed-bed microreactor with a chiral HPLC column for synthesis and on-line separation of enantiomeric products (Scheme 40A). The latter were then analyzed directly by hyphenation of the device to a mass spectrometer *via* electrospray ionization (ESI).

The model Mannich reaction between heptanal and *N*-p-methoxyphenyl (PMP)-protected ethyl iminoglyoxylate catalyzed by silica-supported L-A-Y catalyst proceeded with high *syn*-diastereoselectivity (>10:1 dr) and excellent enantioselectivity (>95% ee_{syn}) (Scheme 40B), in good agreement with results got from off-chip batch experiments (13:1 dr *syn/anti*, >95% ee_{syn}) and literature data.[75]

In parallel, the silica-immobilized H-J organocatalyst was used to study the α-amination of aliphatic aldehydes (propanal, butanal, heptanal, 3-phenylpropanal) with dibenzyl azodicarboxylate (DBAD) (Scheme 40C), but very low conversions were achieved with disparate flow conditions. For this reason, these transformations were run in stop-flow (micro-batch) mode as a mean of extending residence times (1 to 36 min) by infusion and hydraulic entrapping of the reaction mixture inside the reactor for a certain term. With that approach, it has also been possible to study the connection between product formation and residence time at the microscale, shining a light on process productivity as a result of the reactor saturation capacity.

The better result was given by heptanal, with the corresponding α-aminated product obtained in 65% yield, however poor stereocontrol (ca. 50:50 mixture of enantiomers) was observed. Significantly, a single chip could be re-used for a couple of month.

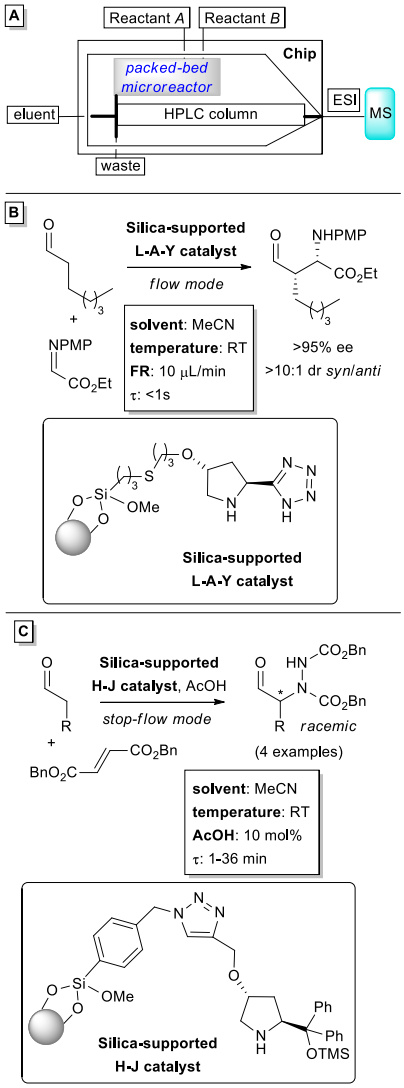

Scheme 40 (A) Schematic representation of an integrated lab-on-a-chip platform for heterogeneous asymmetric organocatalysis. (B) Enantioselective Mannich reaction promoted by silica-supported L-A-Y catalyst. (C) α-Amination of aliphatic aldehydes with DBAD catalyzed by silica-supported H-J catalyst.

An immobilized cinchona-derived picolinamide and a chiral *N*-picolylimidazolidinone promoted the stereoselective reduction of imines with trichlorosilane ($HSiCl_3$) in continuous-flow.

Going more into detail, experiments in batch with *N*-phenyl- and *N*-PMP-protected aryl ketimines using a PS-tethered picolinamide obtained from 9-amino-*epi*-cinchonine yielded (*R*)-configured secondary amine products (up to 98% yield and 87% ee), as shown in Scheme 41A.[76]

The heterogeneous catalyst could be exploited for a maximum of four runs (three recycles), as enantioselectivity clearly decreased (2nd recycle: 67% ee, 3rd recycle: 37% ee).

The $HSiCl_3$-promoted reduction in continuous-flow was studied using the *N*-PMP-protected imine of *p*-nitroacetophenone as the model compound, providing the expected reduction product with 98% yield in an operation time of 50-75 min (Scheme 41B). Yet, enantioselectivity was rather low (44-47% ee) if compared to that observed in the parent batch reactor (85% ee), and diminished over time (20% ee after ca. 3 h performance), most likely due to partial catalyst degradation.

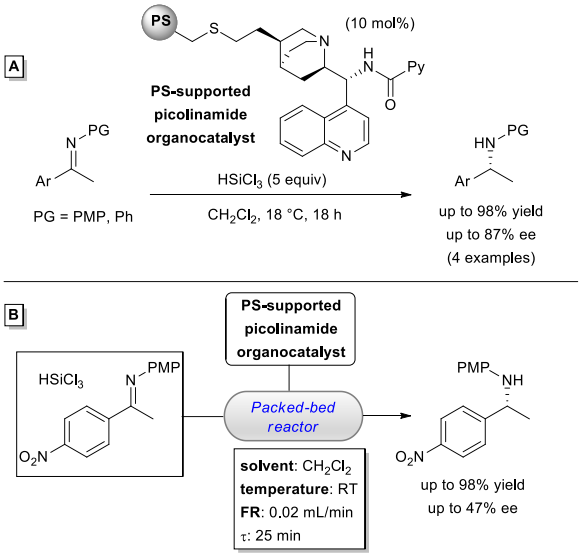

Scheme 41 Stereoselective reduction of imines with $HSiCl_3$ catalyzed by PS-supported cinchona-derived picolinamide. (A) Reaction in batch regime. (B) Reaction in continuous-flow.

Afterwards, a PS-supported chiral *N*-picolylimidazolidinone has been satisfactorily tested in the same type of reaction (Scheme 42).[77]

Successful trials in batch mode provided a diverse set of (*R*)-configured aryl amine compounds with good to high yield (62-99%) and enantioselectivity (up to 97% ee) (Scheme 42A).

It has been shown that the immobilized *N*-picolylimidazolidinone catalyst could work for seven reaction cycles without considerably affecting yield and stereoselectivity (1st cycle: 80% yield, 94% ee; 7th cycle: 76% yield, 87% ee), with maximum 2 h reaction time for each cycle.

These outcomes represented the basis for the development of the related process in continuous-flow. To this aim, fixed-bed reactors packed with the PS-supported *N*-picolylimidazolidinone were prepared and used in the reduction of *N*-PMP imines derived from both acetophenone and 3-benzyloxy acetophenone (Scheme 42B).

In the first case, the reactor guaranteed up to 7 h operation in the production of (*R*)-4-methoxy-*N*-(1-phenylethyl)aniline (Scheme 42B, *red structure*) with high yields (up to 94%), while enantioselectivity was generally good but strictly time-dependent (2 h: 85% ee, 7 h: 73% ee) as a possible result of decomposition of the imidazolidinone catalyst core.

On the other hand, (*R*)-4-methoxy-*N*-{1-[3-(benzyloxy)phenyl]ethyl}-aniline (Scheme 42B, *green structure*) was obtained in 82% yield and 83% ee during the first three

hours of operation, and only slightly lower yield (79%) and enantioselectivity (77% ee) were obtained after six running hours. In this last case, the results acquired take on particular significance considering that the amine obtained is the direct precursor of pharmaceutically relevant (API) compounds, such as rivastigmine (cholinesterase inhibitor), NPS R-568 (calcimimetic) and a KCNQ2 opener with an acrylamide structure (Scheme 42C).

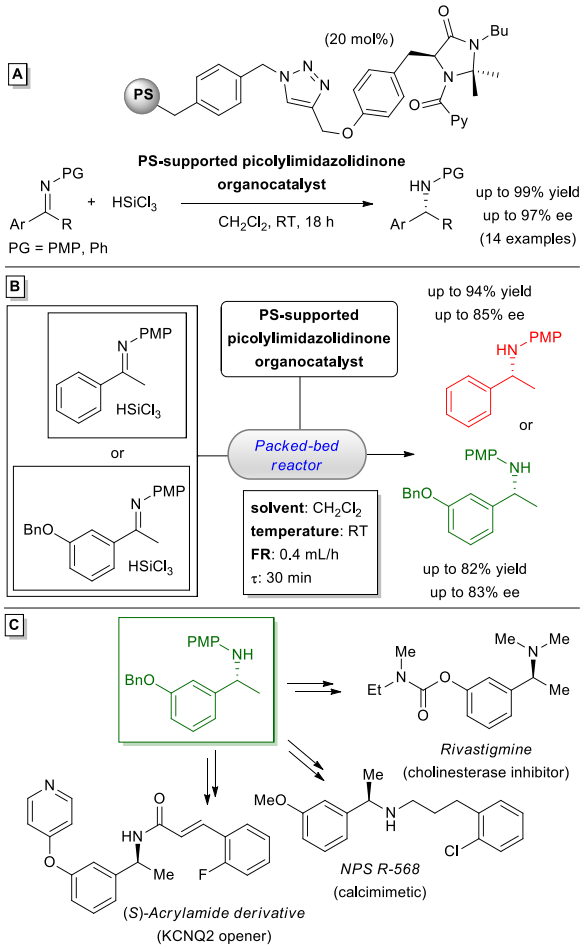

Scheme 42 Stereoselective reduction of imines with $HSiCl_3$ catalyzed by PS-supported chiral *N*-picolylimidazolidinone. (A) Reaction in batch conditions. (B) Reaction in continuous-flow.

It is worth highlighting that the (*R*)-stereocontrol exerted by the heterogenized chiral *N*-picolylimidazolidinone was exactly the same as observed in an identical reaction-type promoted by an analogous homogeneous catalyst.[78] This suggests that the same mechanism may operate in both cases, the preferred (*R*)-enantiomer being formed *via* the favored transition state **19** which minimizes the steric interactions involving both the protecting group at the imine nitrogen atom and the aromatic residue on the imine carbon atom (Figure 3).

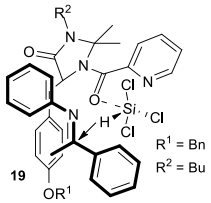

Fig. 3 Favored transition state for the $HSiCl_3$ reduction of imines with PS-supported chiral *N*-picolylimidazolidinone.

Among 4-imidazolidinone catalysts, the first generation MacMillan's one (here abbreviated as MM)[79] was recently supported on silica (carbamate linkage) and evaluated in the Diels-Alder reaction between cyclopentadiene and E-cinnamaldehyde (Scheme 43).[80]

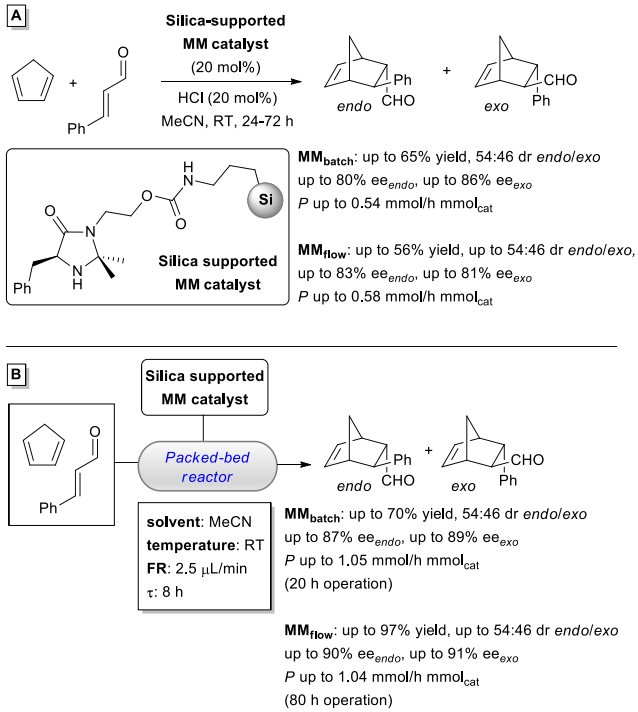

Scheme 43 Diels-Alder reaction between cyclopentadiene and *E*-cinnamaldehyde catalyzed by silica-supported MacMillan (MM) catalyst. (A) Reaction in batch. (B) Continuous-flow process.

Distinguishingly, synthesis/immobilization of the MM catalyst was performed through both batch and continuous-flow strategies, and the heterogeneous organocatalysts obtained in each route (**MM$_{batch}$** and **MM$_{flow}$**) were studied comparatively in the above reaction in both batch and continuous-flow conditions.

Experiments in batch (20 mol% cat., 20 mol% HCl, MeCN, RT, Scheme 43A) presented similar productivities for either catalyst, while efficiencies were a little different. Indeed, **MM$_{batch}$** gave higher cumulated yields of the *endo* and *exo* adducts with increasing reaction time (48 h: 52%, 72 h: 65%) as opposed to **MM$_{flow}$** (48h: 56%, 72 h: 43%), which however furnished a little better enantioselectivities for each single product (48 h: 78% ee$_{endo}$, 80% ee$_{exo}$ *vs* 75% ee$_{endo}$, 78% ee$_{exo}$ given by **MM$_{batch}$**).

The corresponding continuous-flow process (MeCN, RT, FR = 2.5 µL/min, τ = 8 h) took advantage of packed-bed reactors (pre-activated with 0.4 M HCl solution) containing the silica-supported MM catalysts (Scheme 43B). While showing very similar productivities for both **MM$_{batch}$** and **MM$_{flow}$** (ca. 1 mmol/h mmol$_{cat}$), the flow strategy led to assess **MM$_{flow}$** superior in terms of catalytic activity.

As a matter of fact, **MM$_{batch}$** worked efficiently for 20 h, with irreversible loss of catalyst activity observed after that time due to chemical degradation of the solid support. On the contrary, **MM$_{flow}$** showed 7-fold higher lifetime (up to 70-80 h operation time).

This observation demonstrated the possible correlation between the immobilization method and catalyst performances, heterogenization under continuous flow seeming to be the most suitable choice to target catalyst lifetime.

Overall, the continuous-flow cycloaddition reaction promoted by **MM$_{flow}$** gave better stereoselectivities, 2-fold higher productivities and easier-to-handle reaction mixtures by comparison with the parent batch process.

The stereoselective synthesis of optically active chromanones has been conveniently achieved by intramolecular Stetter reactions promoted by the triazolium carbene Rovis catalyst[81] immobilized onto PS (Scheme 44).[82]

Propaedeutic batch trials using the parent PS-supported triazolium salt pre-catalyst and KHMDS as the NHC-forming base gave excellent results (Scheme 44A, R = H, 95% yield, 92% ee) under the well-established reaction conditions for the corresponding homogeneous species (20 mol% cat., 20 mol% base, toluene, RT, 16 h).[83] Unaltered outcomes were obtained by reducing the loading of both catalyst and base by half (10 mol%), thus suggesting that the heterogenized Rovis catalyst had greater activity than the homogeneous counterpart.

With regard to recyclability, enantioselectivity was maintained after ten runs (91% ee), albeit with a slight drop in conversion efficiency after each re-use (5th recycle: 64% yield, 10th recycle: 38% yield), and altogether these data validated the value of the heterogeneous Rovis catalyst (total TON$_{batch}$ = 70).

On these grounds, a wide scope of Michael acceptors has been established (Scheme 44A), giving enantioenriched chromanone derivatives (81-95% ee) in excellent yield (95%), in close analogy with the homogeneous batch results.[83]

Subsequent studies in continuous-flow moved from the use of PS-supported Rovis catalyst as a monolithic microreactor in a two-pump, three-way valve apparatus (Scheme 44B). Unfortunately, the optimized batch conditions have proven ineffective in producing the Stetter adducts, as the strong base KHMDS favored a tandem olefin isomerization-crotonation reaction.[84]

Conversely, the use of triethylamine (2 equiv) as a weaker base for generating the active NHC catalyst resulted in the continuous formation of the predicted chromanone products (91-95% conv., *P* = 0.1-0.3 mmol/h mmol$_{cat}$) with identical enantioselectivity (81-95% ee) to the batch process.

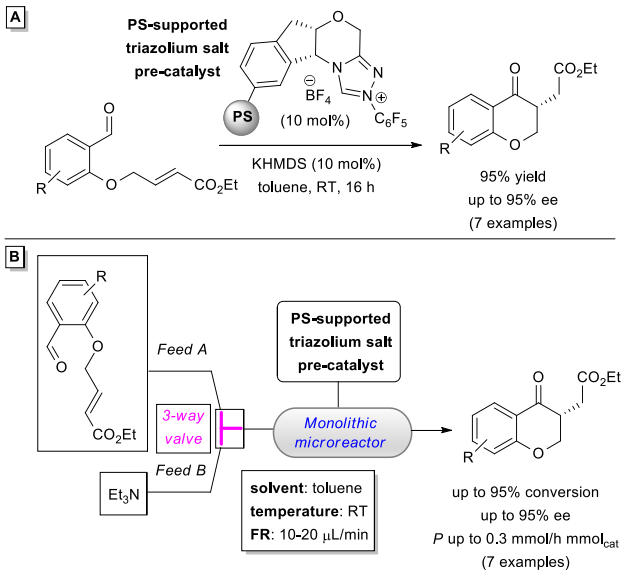

Scheme 44 Stereoselective synthesis of chromanones promoted by PS-supported triazolium carbene Rovis catalyst. (A) Reaction in batch conditions. (B) Reaction in continuous-flow mode.

It is surely to observe that the immobilized Rovis catalyst showed great stability in its monolithic form, providing consistent conversion and stereoselectivity throughout 48 h operation time and only halved productivity after 120 h of use. As result, an accumulated TON$_{flow}$ of 132 and a 2-fold heightening in productivity were found, which demonstrated how advantageous flow mode may be due to the continuous ejection of impurities and moisture from the catalytic bed.

PS-supported enantiopure isothioureas are further examples of heterogeneous organocatalysts that have found application in batch and continuous-flow reactions.

Izquierdo and Pericàs reported an immobilized variant of benzotetramisole (BTM)[85] to achieve the enantioselective synthesis of dihydropyridinones through domino Michael addition/cyclization reactions between chalcone-derived tosylimines and arylacetic acids, in turn activated *in situ* as the corresponding mixed anhydrides (Scheme 45).[86]

Slight modification of a consolidated literature procedure[87] allowed the authors to identify optimal conditions to perform the batch process while preserving the activity of the catalyst, which has been found to depend on the amount of the carboxylic acid-activating species.

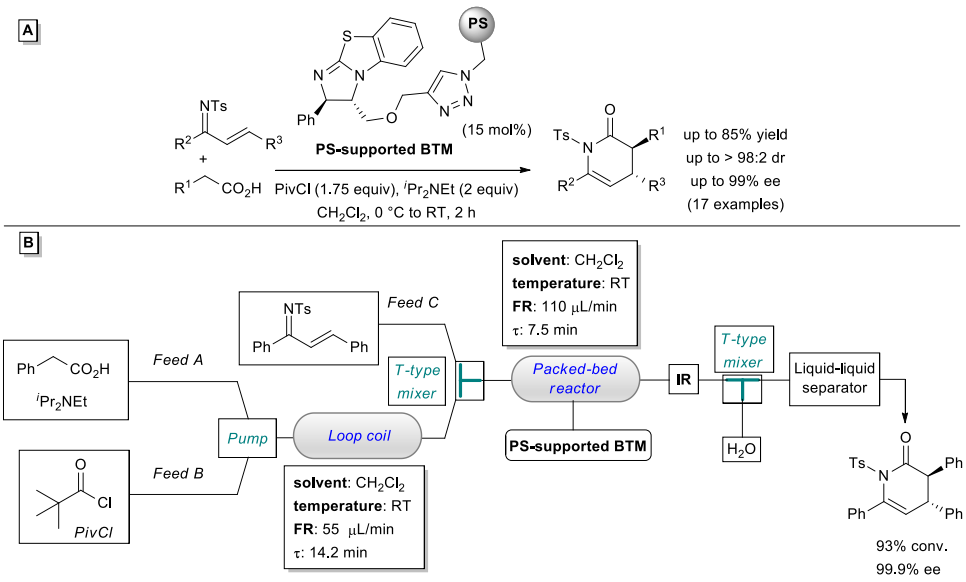

Scheme 45 Enantioselective synthesis of dihydropyridinones through domino Michael addition/cyclization catalyzed by PS-supported BTM. (A) Batch reaction. (B) Continuous-flow process.

Activation of the arylacetic acid with *N*,*N*-diisopropylethylamine (^{i}Pr$_2$NEt, 2 equiv) and pivaloyl chloride (PivCl, 1.75 equiv) followed by reaction with the tosylimine substrate (CH_2Cl_2, 0 °C to RT, 2 h) in the presence of the heterogeneous organocatalyst (15 mol%) produced a wide family of *N*-heterocyclic products with good yields (up to 85%) and excellent stereoselectivities (up to >98:2 dr *trans*/*cis*, up to 99% ee) (Scheme 45A).

No relevant decline of catalytic activity was observed over six successive recycling cycles, as confirmed by a constant enantioselectivity value of 97% and NMR kinetic studies.

A continuous-flow protocol was implemented to carry out the carboxylic acid preactivation and the organocatalytic domino reaction in sequence within the same device. As schematically represented in Scheme 45B for a selected benchmark transformation, the mixed anhydride-forming step occurred inside a loop coil long enough to have full conversion (FR = 55 µL/min, τ = 14.2 min), then the effluent anhydride solution was mixed with pre-formed tosylimine before entering a packed-bed reactor in which the Michael addition/cyclization sequence took place (FR = 110 µL/min, τ = 7.5 min). Downstream liquid-liquid separation aided by suitably conveyed water led to collect continuously organic solutions of the final compound.

After 11 h operation (TON_{flow} = 22.5), the latter was obtained in high conversion (93%, 70% isolated yield) and better enantioselectivity than in the batch process (99.9% ee *vs* 98% ee).

As Scheme 46 depicts, an acyl ammonium ion **20** is initially formed from imine and mixed anhydride reactants. Deprotonation of **20** produces a *Z*-configured ammonium enolate taking part in a stereoselective Michael addition yielding intermediate **21**. Its final intramolecular cyclization gives the dihydropyridinone compound with concomitant catalyst regeneration.

Preferential formation of the *trans*-isomer likely goes through the privileged transition state **22** in the conjugate addition step. This deprives the C-3 bulky substituent on the BTM nucleus of destabilizing steric interactions instead present in the transition state **23** leading to the minor *cis*-isomer.

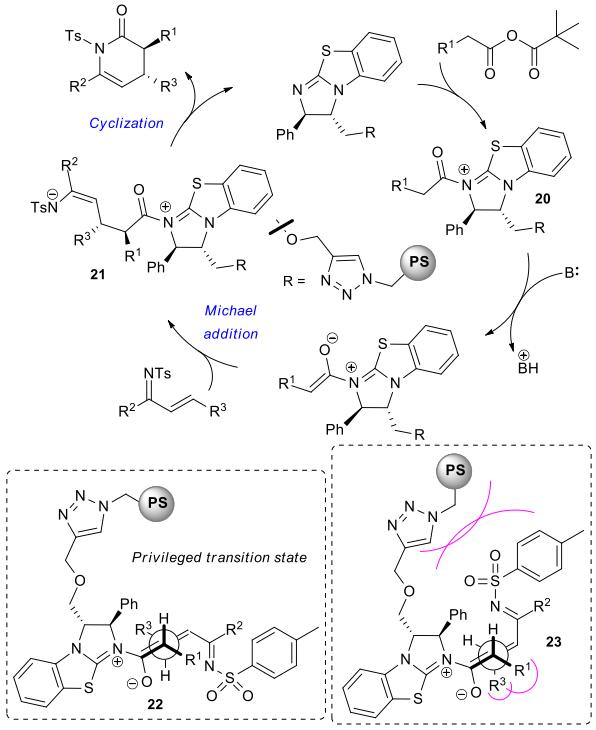

Scheme 46 Tentative organocatalytic cycle for the formation of dihydropyridinone compounds promoted by PS-supported BTM.

A heterogeneous (PS support) isothiourea organocatalyst derived from HyperBTM[88] has been reported to promote the acylative KR of several kinds of secondary alcohols (benzylic/allylic/propargylic alcohols, cycloalkanols, 1,2-diols) with anhydrides (Scheme 47).[89]

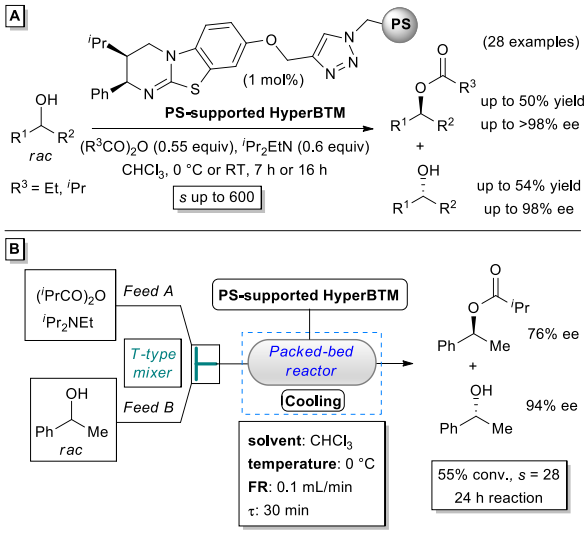

Scheme 47 Acylative KR of secondary alcohols through catalysis by PS-supported HyperBTM. (A) Reaction in batch conditions. (B) Reaction under continuous-flow.

As represented in Scheme 47A, excellent selectivity (*s* factor up to 600) was observed in batch reactions using standard conditions found for the KR of *rac*-1-(naphthalen-2-yl)ethan-1-ol with isobutyric anhydride, which was also used as proving ground for catalyst recyclability.

It has been proved that re-use of the catalyst was possible for 15 cycles without losing activity (TON_{batch} >700), conversion (47%) and selectivity (s ca. 100) being the same for both the 1st cycle and for the 15th one.

Interestingly, re-usability of the recovered catalyst was further assessed for the sequential KR of ten diverse alcohols using either isobutyric or propionic anhydride. Though lower than when using the fresh catalyst, activity and selectivity remained the same throughout the cycles, and importantly, no cross-contamination between cycles was detected.

Based upon these observations, a continuous-flow process (packed-bed reactor) was put in place to effect the KR of *rac*-1-phenylethanol with isobutyric anhydride (Scheme 47B). The right conditions for achieving >50% conversion (FR = 0.1 mL/min, τ = 30 min) could be replicated in five successive reactions (4 mmol scale) with *s* values between 27 and 30 (54-56% conv.). And plus, large-scale (28.8 mmol) processing of the same alcohol within 24 h led to recover the (*R*)-enantiomer in 40% yield (55% conv.) with 94% ee (*s* = 28).

Just as important is that the already used reactor made it possible to kinetically resolve selected benzylic, allylic, propargylic alcohols and cycloalkanols (nine alcohol/anhydride combinations at 4 mmol scale) with excellent levels of conversion (up to 63%) and selectivity (*s* up to 200), with the enantioenriched alcohol isolated in up to 98% ee.

Again, the use of the same reactor with diverse anhydrides and alcohols did not provide any evidence of catalyst deactivation or cross-contamination.

Markedly, the same batch of catalyst could be used for all tests in continuous-flow (>100 h operation time), demonstrating very unique robustness of PS-supported HyperBTM.

4. Conclusions

The overall picture that emerges from the analysis of recent literature on organocatalyzed reactions under continuous-flow confirms the peculiarity of flow chemistry as enabling technique able to fulfill the mission of process intensification, also going to meet the demands of sustainability.

In most cases, the continuous-flow approach gave the chance to widen the range of reaction conditions for a specific transformation, an even greater implementation being achieved by in-line addition of processing units (for e.g. reaction monitoring/analysis, extraction and/or separation),[21,27,41,70,74,86] as well as by integration of multiple reactors (compartmentalization) for the telescoping of different chemical events.[21,27,56,70,86]

Compared with the works published until 2015, it should be stressed that organocatalysis in continuous-flow has somehow grown: some of the methods developed have a good scope of substrates and new types of starting materials (based on biomass) have been effectively processed,[27,50,54] whilst activation modes seem to still be quite few.

However, it should not be denied that some problems still remain, the main one being catalyst deactivation (specially in the case of supported organocatalysts), which may lessen reaction efficiency and hamper large-scale process transfer.

In this matter, a potential solution could be to target the lifetime of the catalyst by choosing accurately the strategy for its synthesis and immobilization (batch *vs* continuous-flow mode).[80]

Not the least is that immobilized organocatalysts in the form of monolithic reactors could represent a possible solution for easy scale-up at an industrial level (relative to the analogous packed-bed reactors), thanks to their better flow properties.[14]

In addition, a new road could also be traced using a non-conventional strategy for heterogeneous flow synthesis, through bed-type systems based on homogeneous organocatalysts which do not dissolve in the flowing solvents.[68]

On these points, we are convinced that continuous-flow organocatalysis will see further development, making inroads to new (intensified) processes amenable to large-scale production of industrially relevant (chiral) products such as fine chemicals, pharmaceuticals, agrochemicals, and bioactive natural compounds.

Conflicts of interest

There are no conflicts to declare.

References

1 For selected reviews on flow chemistry, see: *(a)* S. V. Luis and E. Garcia-Verdugo, *Flow Chemistry: Integrated Approaches for Practical Applications* (Green Chemistry Series), Royal Society of Chemistry, Cambridge, 2020; *(b)* M. B. Plutschack, B. Pieber, K. Gilmore and P. H. Seeberger, *Chem. Rev.*, 2017, **117**, 11796; *(c)* J. Britton and C. L. Raston, *Chem. Soc. Rev.*, 2017, **46**, 1250; *(d)* F. Darvas, G. Dormán and V. Hessel, *Flow Chemistry*, De Gruyter, Berlin, 2014; *(e)* K. F. Jensen, B. J. Reizman and S. G. Newman, *Lab. Chip*, 2014, **14**, 3206; *(f)* K. S. Elvira, X. Casadevall i Solvas, R. C. R.Wootton and A. J. deMello, *Nat. Chem.*, 2013, **5**, 905; *(g)* D. T. McQuade and P. H. Seeberger, *J. Org. Chem.*, 2013, **78**, 6384; *(h)* J. C. Pastre, D. L. Browne and S. V. Ley, *Chem. Soc. Rev*., 2013, **42**, 8849; *(i)* T. Wirth, *Microreactors in Organic Chemistry and Catalysis*, 2nd Edition, Wiley-VCH, Weinheim, 2013; *(j)* I. R. Baxendale, *J. Chem. Technol. Biotechnol.*, 2013, **88**, 519; *(k)* V. Hessel, D. Kralisch, N. Kockmann, T. Noël and Q. Wang, *ChemSusChem*, 2013, **6**, 746; *(l)* I. R. Baxendale, L. Brocken and C. J. Mallia, *Green Process. Synth.*, 2013, **2**, 211; *(m)* C. Wiles and P. Watts, *Green Chem.* 2012, **14**, 38; *(n)* J. Wegner, S. Ceylan and A. Kirschning, *Chem. Commun.*, 2011, **47**, 4583; *(o)* R. L. Hartman, J. P. McMullen and K. F. Jensen, *Angew. Chem. Int. Ed.*, 2011, **50**, 7502; *(p)* C.Wiles and P. Watts, *Chem. Commun.* 2011, **47**, 6512; *(q)* C. Wiles and P. Watts, *Micro Reaction Technology in Organic Synthesis*; CRC Press, 2011; *(r)* V. Hessel, *Chem. Eng. Technol.*, 2009, **32**, 1655; *(s)* S. V. Luis and E. García-Verdugo, *Chemical Reactions and Processes under Flow Conditions*, RSC Publishing, Cambridge, 2009.

2 J. Wegner, S. Ceylan and A. Kirschning, *Adv. Synth. Catal.*, 2012, **354**, 17.

3 *(a)* S. Rossi, A. Puglisi and M. Benaglia, *ChemCatChem*, 2018, **10**, 1512; *(b)* S. Rossi, M. Benaglia, D. Brenna, R. Porta and M. Orlandi, *J. Chem. Educ.*, 2015, **13**, 1398.

4 *(a)* A. Nagaki, K. Sasatsuki, S. Ishiuchi, N. Miuchi, M. Takumi and J.-i. Yoshida, *Chem. – Eur. J.*, 2019, **25**, 4946; *(b)* J.-i. Yoshida, H. Kim and A. Nagaki, *J. Flow Chem.*, 2017, **7**, 60; *(c)* J.-i. Yoshida, *Flash Chemistry: Fast Organic Synthesis in Microsystems*, Wiley, New York, 2008.

5 *(a)* A. Basile, A. Iulianelli and S. Liguori, in *Sustainable Development in Chemical Engineering – Innovative Technologies,* ed. V. Piemonte, M. De Falco and A. Basile, Wiley, New York, 1st Edition, 2013, Chapter 6, pp. 119-151; *(b)* A. Górak and A. Stankiewicz, *Annu. Rev. Chem. Biomol. Eng.*, 2011, **2**, 431.

6 For selected reviews on the inter-relation between flow chemistry and green chemistry/sustainable chemical processes, see: *(a)* L. Rogers and K. F. Jensen, *Green Chem.*, 2019, **21**, 3481; *(b)* R. Gérardy, R. Morodo, J. Estager, P. Luis, D. P. Debecker and J.‑C. M. Monbaliu, *Top. Curr. Chem.*, 2019, **377**, 1; *(c)* J. Yue, *Catal. Today*, 2018, **308**, 3; *(d)* R. Gérardy, N. Emmanuel, T. Toupy, V.-E. Kassin, N. N. Tshibalonza, M. Schmitz and J.-C. M. Monbaliu, *Eur. J. Org. Chem.*, 2018, 2301; *(e)* F. Fanelli, G. Parisi, L. Degennaro and R. Luisi, *Beilstein J. Org. Chem.*, 2017, **13**, 520; *(f)* L. Vaccaro, *Sustainable Flow Chemistry: Methods and Applications*, Wiley-VCH, , Weinheim, 2017; *(g)* L. Vaccaro, D. Lanari, A. Marrocchi and G. Strappaveccia, *Green Chem.*, 2014, **16**, 3680; *(h)* S. G. Newman and K. F. Jensen, *Green Chem.*, 2013, **15**, 1456; *(i)* S. V. Ley, *Chem. Rec.*, 2012, **12**, 378; *(j)* J.-i. Yoshida, H. Kim and A. Nagaki, *ChemSusChem*, 2011, **4**, 331.

7 US Government Accountability Office, GAO-18-307, February 2018. Available on line: https://www.gao.gov/products/GAO-18-307 (accessed on 14 February 2020).

8 C. Jiménez-González, P. Poechlauer, Q. B. Broxterman, B.-S. Yang, D. am Ende, J. Baird, C. Bertsch, R. E. Hannah, P. Dell'Orco, H. Noorman, S. Yee, R. Reintjens, A. Wells, V. Massonneau and J. Manley, *Org. Process Res. Dev.*, 2011, **15**, 900.

9 For selected papers on continuous-flow manufacturing of API, see: *(a)* D. Riley, I. Strydom, R. Chikwamba and J.-L. Panayides, *React. Chem. Eng.*, 2019, **4**, 457; *(b)* A. R. Bogdan and A. W. Dombrowski, *J. Med. Chem.*, 2019, **62**, 6422-6468; *(c)* M. Köckinger, C. A. Hone, B. Gutmann, P. Hanselmann, M. Bersier, A. Torvisco and C. O. Kappe, *Org. Process Res. Dev.*, 2018, **22**, 1553; *(d)* R. E. Ziegler, B. K. Desai, J.-A. Jee, B. F. Gupton, T. D. Roper and T. F. Jamison, *Angew. Chem. Int. Ed.*, 2018, **57**, 7181; *(e)* D. Geier, P. Schmitz, J. Walkowiak, W. Leitner and G. Franciò, *ACS Catal.*, 2018, **8**, 3297; *(f)* M. J. Pedersen, T. Skovby, M. J. Mealy, K. Dam-Johansen and S. Kiil, *Org. Process Res. Dev.*, 2018, **22**, 228; *(g)* D. L. Hughes, *Org. Process Res. Dev.*, 2018, **22**, 13; *(h)* R. O. M. A. de Souza and P. Watts, *J. Flow Chem.*, 2017, **7**, 146; *(i)* P. Bana, R. Örkényi, K. Lövei, Á. Lakó, G. I. Túrós, J. Éles, F. Faigl and I. Greiner, *Bioorg. Med. Chem.*, 2017, **25**, 6180; *(j)* L. Pellegatti, A. Hafner and J. Sedelmeier, *J. Flow Chem.*, 2016, **6**, 198; *(k)* Z. Amara, M. Poliakoff, R. Duque, D. Geier, G. Franciò, C. M. Gordon, R. E. Meadows, R. Woodward and W. Leitner, *Org. Process Res. Dev.*, 2016, **20**, 1321; *(l)* R. Porta, M. Benaglia and A. Puglisi, *Org. Process Res. Dev.*, 2016, **20**, 2; *(m)* B. Gutmann, D. Cantillo and C. O. Kappe, *Angew. Chem. Int. Ed.* 2015, **54**, 6688; *(n)* M. Baumann and I. R. Baxendale, *Beilstein J. Org. Chem.*, 2015, **11**, 1194.

10 For a seminal example of industrial continuous manufacturing of an API, see: *(a)* P. L. Heider, S. C. Born, S. Basak, B. Benyahia, R. Lakerveld, H. Zhang, R. Hogan, L. Buchbinder, A. Wolfe, S. Mascia, J. M. B. Evans, T. F. Jamison and K. F. Jensen, *Org. Process Res. Dev.*, 2014, **18**, 402; *(b)* S. Mascia, P. L. Heider, H. Zhang, R. Lakerveld, B. Benyahia, P. I. Barton, R. D. Braatz, C. L. Cooney, J. M. B. Evans, T. F. Jamison, K. F. Jensen, A. S. Myerson and B. L. Trout, *Angew. Chem. Int. Ed.*, 2013, **52**, 12359.

11 *(a)* J. Woodcock, *Modernizing Pharmaceutical Manufacturing – Continuous Manufacturing as a Key Enabler*; Lecture presented at the MIT-CMAC International Symposium on Continuous Manufacturing of Pharmaceuticals, Cambridge, MA, USA, 20 May 2014; *(b)* D. Hernán, *Continuous Manufacturing: Challenges and Opportunities. EMA Perspective*; Lecture presented at the 3rd FDA/PQRI Conference on Advancing Product Quality: Rockville, MD, USA, 22–24 March 2017.

12 For selected reviews on organocatalysis, see: *(a)* A. Sinibaldi, V. Nori, A. Baschieri, F. Fini, A. Arcadi and A. Carlone, *Catalyst*s, 2019, **9**, 928; *(b)* V. d. G. Oliveira, M. F. d. C. Cardoso and L. d. S. M. Forezi, *Catalysts*, 2018, **8**, 605; *(c)* P. Vogel, Y.-h. Lam, A. Simon and K. N. Houk, *Catalysts*, 2016, **6**, 128; *(d)* J. Aleman and S. Cabrera, *Chem. Soc. Rev.*, 2013, **42**, 774; *(e)* S. Bertelsen and K. A. Jørgensen, *Chem. Soc. Rev.*, 2009, **38**, 2178; *(f)* D. W. C. MacMillan, *Nature*, 2008, **455**, 304; *(g)* P. Melchiorre, P. Marigo, A. Carlone and G. Bartoli, *Angew. Chem. Int. Ed*., 2008, **47**, 6138; *(h)* P. I. Dalko and L. Moisan, *Angew. Chem. Int. Ed.*, 2004, **43**, 5138.

13 *(a)* A. M. Hafez, A. E. Taggi, T. Dudding and T. Lectka, *J. Am. Chem. Soc.*, 2001, **123**, 10853; *(b)* A. M. Hafez, A. E. Taggi, H. Wack, W. J. Drury III and T. Lectka, *Org. Lett.*, 2000, **2**, 3963.

14 *(a)* T. Wirth, *Microreactors in Organic Chemistry and Catalysis*, 2nd Edition, Wiley-VCH, Weinheim, 2013; *(b)* G. Jas and A. Kirschning, *Chem. – Eur. J.*, 2003, **9**, 5708; *(c)* A. Stankiewicz, *Chem. Eng. Sci.*, 2001, **56**, 359; *(d)* R. M. Heck, S. Gulati and R. J. Farrauto, *Chem. Eng. J.*, 2001, **82**, 149.

15 For selected reviews on catalysis in continuous-flow, see: *(a)* H. Ishitani, Y. Saito, B. Laroche, X. Rao and S. Kobayashi, in *Flow Chemistry: Integrated Approaches for Practical Applications*, ed. S. V. Luis and E. Garcia-Verdugo, The Royal Society of Chemistry, Cambridge, 2020, Chapter 1, pp. 1-49;

(b) K. Masuda, T. Ichitsuka, N. Koumura, K. Sato and S. Kobayashi, *Tetrahedron*, 2018, **74**, 1705; *(c)* C. Rodríguez-Escrich and M. A. Pericàs, *Chem. Rec.*, 2019, **19**, 1872; *(d)* R. Ciriminna, M. Pagliaro and R. Luque, *Preprints*, 2019, 2019010175 (DOI: 10.20944/preprints201901.0175.v1); *(e)* M. Colella, C. Carlucci and R. Luisi, *Top. Curr. Chem.*, 2018, **376**, 46; *(f)* R. Munirathinam, J. Huskens and W. Verboom, *Adv. Synth. Catal.*, 2015, **357**, 1093; *(g)* A. Puglisi, M. Benaglia and V. Chiroli, *Green Chem.*, 2013, **15**, 1790; *(h)* D. Zhao and K. Ding, *ACS Catal.*, 2013, **3**, 928; *(i)* T. Tsubogo, T. Ishiwata and S. Kobayashi, *Angew. Chem. Int. Ed.*, 2013, **52**, 6590; *(j)* X. Y. Mak, P. Laurino and P. H. Seeberger, *Beilstein J. Org. Chem.*, 2009, **5**, No. 19, DOI:10.3762/bjoc.5.19.

16 *(a)* A. Puglisi, M. Benaglia, R. Porta and F. Coccia, *Curr. Organocatal.*, 2015, **2**, 79; *(b)* F. G. Finelli, L. S. M. Miranda and R. O. M. A. de Souza, *Chem. Commun.*, 2015, **51**, 3708; *(c)* I. Atodiresei, C. Vila and M. Rueping, *ACS Catal.*, 2015, **5**, 1972; *(d)* C. Rodríguez-Escrich and M. A. Pericàs, *Eur. J. Org. Chem.*, 2015, 1173.

17 D. J. M. Lyons, R. D. Crocker, D. Enders and T. V. Nguyen, *Green Chem.*, 2017, **19**, 3993.

18 M. Fochi, L. Caruana and L. Bernardi, *Synthesis*, 2014, **46**, 135.

19 J. Liu, J. Xu, Z. Li, Y. Huang, H. Wang, Y. Gao, T. Guo, P. Ouyang and K. Guo, *Eur. J. Org. Chem.*, 2017, 3996.

20 *(a)* Q. Ren, M. Li, L. Yuan and J. Wang, *Org. Biomol. Chem.*, 2017, **15**, 4731; *(b)* D. M. Flanigan, F. Romanov-Michailidis, N. A. White and T. Rovis, *Chem. Rev.* 2015, **115**, 9307.

21 L. Di Marco, M. Hans, L. Delaude and J.-C. M. Monbaliu, *Chem. – Eur. J.*, 2016, **22**, 4508.

22 *(a)* R. Singh, R. M. Kissling, M.-A. Letellier and S. P. Nolan, *J. Org. Chem.*, 2004, **69**, 209; *(b)* G. A. Grasa, T. Güveli, R. Singh and S. P. Nolan, *J. Org. Chem.*, 2003, **68**, 2812; *(c)* G. A. Grasa, R. M. Kissling and S. P. Nolan, *Org. Lett.*, 2002, **4**, 3583.

23 G. W. Nyce, J. A. Lamboy, E. F. Connor, R. M. Waymouth and J. L. Hedrick, *Org. Lett.*, 2002, **4**, 3587.

24 Y. Wang and Z. Li, *Chin. J. Catal.*, 2012, **33**, 502.

25 S. S. Abubakar, M. Benaglia, S. Rossi and R. Annunziata, *Catal. Today*, 2018, **308**, 94.

26 S. E. Denmark, S. Rossi, M. P. Webster and H. Wang, *J. Am. Chem. Soc.*, 2014, **136**, 13016.

27 R. Morodo, R. Gérardy, G. Petit and J.-C. M. Monbaliu, *Green Chem.*, 2019, **21**, 4422.

28 E. Santacesaria, R. Vitiello, R. Tesser, V. Russo, R. Turco and M. Di Serio, *Ind. Eng. Chem. Res.*, 2014, **53**, 8939.

29 P. Lecomte and R. Jerome, in *Encyclopedia of Polymer Science and Technol*ogy, ed. H. F Mark, Wiley, New York, 4th Edition, 2014, 12, 137-156.

30 *(a)* R. C. Pratt, B. G. G. Lohmeijer, D. A. Long, R. M. Waymouth and J. L. Hedrick, *J. Am. Chem. Soc.*, 2006, **128**, 4556; *(b)* B. G. G. Lohmeijer, R. C. Pratt, F. Leibfarth, J. W. Logan, D. A. Long, A. P. Dove, F. Nederberg, J. Choi, C. Wade, R. M. Waymouth and J. L. Hedrick, *Macromolecules*, 2006, **39**, 8574.

31 N. Zhu, W. Feng, X. Hu, Z. Zhang, Z. Fang, K. Zhang, Z. Li and K. Guo, *Polymer*, 2016, **84**, 391.

32 S. A. van den Berg, H. Zuilhof and T. Wennekes, *Macromolecules*, 2016, **49**, 2054.

33 H. W. Horn, G. O. Jones, D. S. Wei, K. Fukushima, J. M. Lecuyer, D. J. Coady, J. L. Hedrick and J. E. Rice, *J. Phys. Chem. A*, 2012, **116**, 12389.

34 M. R. Karver, R. Weissleder and S. A. Hilderbrand, *Bioconjugate Chem.*, 2011, **22**, 2263.

35 K. Matyjaszewski and J. Xia, *Chem. Rev.*, 2001, **101**, 2921.

36 B. L. Ramsey, R. M. Pearson, L. R. Beck and G. M. Miyake, *Macromolecules*, 2017, **50**, 2668.

37 X. Pan, C. Fang, M. Fantin, N. Malhotra, W. Y. So, L. A. Peteanu, A. A. Isse, A. Gennaro, P. Liu and K. Matyjaszewski, *J. Am. Chem. Soc.*, 2016, **138**, 2411.

38 G. Ramakers, A. Krivcov, V. Trouillet, A. Welle, H. Möbius and T. Junkers, *Macromol. Rapid Commun.*, 2017, **38**, 1700423.

39 M. Raj, V. Maya, S. K. Ginotra and V. K. Singh, *Org. Lett.*, 2006, **8**, 4097.

40 L. Schober, S. Ratnam, Y. Yamashita, N. Adebar, M. Pieper, A. Berkessel, V. Hessel and H. Gröger, *Synthesis*, 2019, **51**, 1178.

41 P. Kisszekelyi, A. Alammar, J. Kupai, P. Huszthy, J. Barabas, T. Holtzl, L. Szente, C. Bawn, R. Adams and G. Szekely, *J. Catal.*, 2019, **371**, 255.

42 P. J. Dyson and P. G. Jessop, *Catal. Sci. Technol.*, 2016, **6**, 3302.

43 S. Ceylan, H. C.-H. Law, A. Kirschning and P. H. Toy, *Synthesis*, 2017, **49**, 145.

44 *(a)* C. Guo and X. Lu, *J. Chem. Soc., Perkin Trans. 1*, 1993, 1921; *(b)* B. M. Trost and U. Kazmaier, *J. Am. Chem. Soc.*, 1992, **114**, 7933.

45 P. Ranjan, G. M. Ojeda, U. K. Sharma and E. V. Van der Eycken, *Chem. – Eur. J.*, 2019, **25**, 2442.

46 J. Ametovski, U. Dutta, L. Burchill, D. Maiti, D. W. Lupton and J. F. Hooper, *Chem. Commun.*, 2017, **53**, 13071.

47 A. Zaghi, D. Ragno, G. Di Carmine, C. De Risi, O. Bortolini, P. P. Giovannini, G. Fantin and A. Massi, *Beilstein J. Org. Chem.*, 2016, **12**, 2719.

48 D. Ragno, A. Zaghi, G. Di Carmine, P. P. Giovannini, O. Bortolini, M. Fogagnolo, A. Molinari, A. Venturini and A. Massi, *Org. Biomol. Chem.*, 2016, **14**, 9823.

49 M. Asadi, J. F. Hooper and D. W. Lupton, *Tetrahedron*, 2016, **72**, 3729.

50 D. Ragno, A. Brandolese, D. Urbani, G. Di Carmine, C. De Risi, O. Bortolini, P. P. Giovannini and A. Massi, *React. Chem. Eng.*, 2018, **3**, 816.

51 *(a)* A. Axelsson, A. Antoine-Michard and H. Sundén, *Green Chem.*, 2017, **19**, 2477; *(b)* A. Axelsson, E. Hammarvid, L. Ta and H. Sundén, *Chem. Commun.*, 2016, **52**, 11571.

52 J. Piera and J.-E. Bäckvall, *Angew. Chem. Int. Ed.*, 2008, **47**, 3506.

53 O. Bortolini, A. Cavazzini, P. Dambruoso, P. P. Giovannini, L. Caciolli, A. Massi, S. Pacifico and D. Ragno, *Green Chem.*, 2013, **15**, 2981.

54 A. Brandolese, D. Ragno, G. di Carmine, T. Bernardi, O. Bortolini, P. P. Giovannini, O. Ginoble Pandoli, A. Altomare and A. Massi, *Org. Biomol. Chem.*, 2018, **16**, 8955.

55 Y. Orihashi, M. Nishikawa, H. Ohno, E. Tsuchida, H. Matsuda, H. Nakanishi and M. Kato, *Bull. Chem. Soc. Jpn.*, 1987, **60**, 3731.

56 E. Peris, R. Porcar, M. I. Burguete, E. García-Verdugo and S. V. Luis, *ChemCatChem*, 2019, **11**, 1955.

57 *(a)* F. Giacalone and M. Gruttadauria, *ChemCatChem*, 2016, **8**, 664; *(b)* R. Fehrmann, A. Riisager and M. Haumann, *Supported Ionic Liquids: Fundamentals and Applications*, Wiley-VCH, Weinheim, 2014; *(c)* H. Li, P. S. Bhadury, B. Song and S. Yang, *RSC Adv.*, 2012, **2**, 12525; *(d)* C. Van Doorslaer, J. Wahlen, P. Mertens, K. Binnemans and D. De Vos, *Dalton Trans.*, 2010, **39**, 8377.

58 *(a)* A. Sarkar, S. R. Roy and A. K. Chakraborti, *Chem. Commun.*, 2011, **47**, 4538; *(b)* L. Zhang, X. Fu and G. Gao, *ChemCatChem*, 2011, **3**, 1359; *(c)* S. R. Roy and A. K. Chakraborti, *Org. Lett.*, 2010, **12**, 3866; *(d)* A. Aggarwal, N. L. Lancaster, A. R. Sethi and T. Welton, *Green Chem.*, 2002, **4**, 517.

59 S. Hoffmann, A. M. Seayad and B. List, *Angew. Chem. Int. Ed.*, 2005, 7424.

60 L. Clot-Almenara, C. Rodríguez-Escrich, L. Osorio-Planes and M. A. Pericàs, *ACS Catal.*, 2016, **6**, 7647.

61 P. Jain and J. C. Antilla, *J. Am. Chem. Soc.*, 2010, **132**, 11884.

62 S. Cañellas, C. Ayats, A. H. Henseler and M. A. Pericàs, *ACS Catal.*, 2017, **7**, 1383.

63 *(a)* Z. G. Hajos and D. R. Parrish, *J. Org. Chem.*, 1974, **39**, 1615; *(b)* U. Eder, G. Sauer and R. Wiechert, *Angew. Chem. Int. Ed.*, 1971, **10**, 496.

64 *(a)* S. Luo, C. Xu and L. Zhang, Can. Patent CN 10355931A 2014; *(b)* C. Xu, L. Zhang, P. Zhou, S. Luo and J.-P. Cheng, *Synthesis*, 2013, **45**, 1939; *(c)* P. Zhou, L. Zhang, S. Luo and J.-P. Cheng, *J. Org. Chem.*, 2012, **77**, 2526.

65 *(a)* E. Nakashima and H. Yamamoto, *Chem. Asian J.*, 2017, **12**, 41; *(b)* A. Hartikka and P. I. Arvidsson, *Tetrahedron: Asymmetry*, 2004, **15**, 1831; *(c)* A. J. Cobb, D. M. Shaw and S. V. Ley, *Synlett*, 2004, 558; *(d)* H. Torii, M. Nakadai, K. Ishihara, S. Saito and H. Yamamoto, *Angew. Chem. Int. Ed.*, 2004, **43**, 1983.

66 R. Greco, L. Caciolli, A. Zaghi, O. Pandoli, O. Bortolini, A. Cavazzini, C. De Risi and A. Massi, *React. Chem. Eng.*, 2016, **1**, 183.

67 *(a)* O. Bortolini, L. Caciolli, A. Cavazzini, V. Costa, R. Greco, A. Massi and L. Pasti, *Green Chem.*, 2012, **14**, 992; *(b)* F. E. Valera, M. Quaranta, A. Moran, J. Blacker, A. Armstrong, J. T. Cabral and D. G. Blackmond, *Angew. Chem. Int. Ed.*, 2010, **49**, 2478.

68 E. Nakashima and H. Yamamoto, *Chem. – Eur. J.*, 2018, **24**, 1076.

69 *(a)* B. S. Donslund, T. K. Johansen, P. H. Poulse, K. S. Halskov and K. A. Jørgensen, *Angew. Chem. Int. Ed.*, 2015, **54**, 13860; *(b)* K. L. Jensen, G. Dickmeiss, H. Jiang, Ł. Albrecht and K. A. Jørgensen, *Acc. Chem. Res.*, 2012, **45**, 248; *(c)* A. Mielgo and C. Palomo, *Chem. – Asian J.*, 2008, **3**, 922.

70 P. Llanes, C. Rodríguez-Escrich, S. Sayalero and M. A. Pericàs, *Org. Lett.*, 2016, **18**, 6292.

71 J. Lai, S. Sayalero, A. Ferrali, L. Osorio-Planes, F. Bravo, C. Rodríguez-Escrich and M. A. Pericàs, *Adv. Synth. Catal.*, 2018, **360**, 2914.

72 S. B. Ötvös, M. A. Pericàs and C. O. Kappe, *Chem. Sci.*, 2019, **10**, 11141.

73 P. Szcześniak, S. Buda, L. Lefevre, O. Staszewska-Krajewska and J. Mlynarski, *Eur. J. Org. Chem.*, 2019, 6973.

74 R. Warias, A. Zaghi, J. J. Heiland, S. K. Piendl, K. Gilmore, P. H. Seeberger, A. Massi and D. Belder, *ChemCatChem*, 2018, **10**, 5382.

75 *(a)* A. Odedra and P. H. Seeberger, *Angew. Chem. Int. Ed.*, 2009, **48**, 2699; *(b)* A. Ting and S. E. Schaus, *Eur. J. Org. Chem.*, 2007, 5797.

76 S. D. Fernandes, R. Porta, P. C. Barrulas, A. Puglisi, A. J. Burke and M. Benaglia, *Molecules*, 2016, **21**, 1182.

77 R. Porta, M. Benaglia, R. Annunziata, A. Puglisi and G. Celentano, *Adv. Synth. Catal.*, 2017, **359**, 2375.

78 D. Brenna, R. Porta, E. Massolo, L. Raimondi and M. Benaglia, *ChemCatChem*, 2017, **9**, 941.

79 K. A. Ahrendt, C. J. Borths and D. W. C. MacMillan, *J. Am. Chem. Soc.*, 2000, **122**, 4243.

80 P. H. R. de Oliveira, B. M. da S. Santos, R. A. C. Leão, L. S. M. Miranda, R. A. S. San Gil, R. O. M. A. de Souza and F. G. Finelli, *ChemCatChem*, 2019, **21**, 5553.

81 M. S. Kerr and T. Rovis, *J. Am. Chem. Soc.*, 2004, **126**, 8876.

82 D. Ragno, G. Di Carmine, A. Brandolese, O. Bortolini, P. P. Giovannini and A. Massi, *ACS Catal.*, 2017, **7**, 6365.

83 J. R. de Alaniz, M. S. Kerr, J. L. Moore and T. Rovis, *J. Org. Chem.*, 2008, **73**, 2033.

84 E. Ciganek, *Synthesis*, 1995, **1995**, 1311.

85 V. B. Birman and X. Li, *Org. Lett.*, 2006, **8**, 1351.

86 J. Izquierdo and M. A. Pericàs, *ACS Catal.*, 2016, **6**, 348.

87 C. Simal, T, Lebl, A. M. Z. Slawin and A. D. Smith, *Angew. Chem. Int. Ed.*, 2012, **51**, 3653.

88 *(a)* A. Matviitsuk, M. D. Greenhalgh, D.-J. B. Antúnez, A. M. Z. Slawin and A. D. Smith, *Angew. Chem. Int. Ed.*, 2017, **56**, 12282; *(b)* E. R. T. Robinson, C. Fallan, C. Simal, A. M. Z. Slawin and A. D. Smith, *Chem. Sci.*, 2013, **4**, 2193; *(c)* D. Belmessieri, L. C. Morrill, C. Simal, A. M. Z. Slawin and A. D. Smith, *J. Am. Chem. Soc.*, 2011, **133**, 2714; *(d)* C. Joannesse, C. P. Johnston, C. Concellón, C. Simal, D. Philp and A. D. Smith, *Angew. Chem. Int. Ed.*, 2009, **48**, 8914.

89 R. M. Neyyappadath, R. Chisholm, M. D. Greenhalgh, C. Rodríguez-Escrich, M. A. Pericàs, G. Hähner and A. D. Smith, *ACS Catal.*, 2018, **8**, 1067.